ERA-40 Project Report Series

No. 24 Validation of the hydrological cycle of ERA-40

Stefan Hagemann, Klaus Arpe and Lennart Bengtsson

Series: ECMWF ERA-40 Project Report Series

A full list of ECMWF Publications can be found on our web site under:
http://www.ecmwf.int/publications/

Contact: library@ecmwf.int

European Centre for Medium Range Weather Forecasts
Shinfield Park, Reading, RG2 9AX, England

ERA-40 Project Report Series No. 24

Validation of the hydrological cycle of ERA-40

Stefan Hagemann[1], Klaus Arpe[1] and Lennart Bengtsson [1,2]

June 2005

[1] Current affiliation:
[1]Max Planck Institute for Meteorology, Bundesstraße 53
D-20146 Hamburg, Germany

[2] Environmental Systems Science Centre
Harry Pitt Building, Whiteknights, PO Box 238, Reading RG6 6AL, UK

Contents

Abstract

The European Centre for Medium-Range Weather Forecasts (ECMWF) has prepared a new 40 year reanalysis dataset (ERA40). Based on the observational data that were used, the whole ERA40 time period 1958-2001 can be divided into three parts: the satellite period 1989-2001 when a large amount of satellite data were assimilated into the ERA40 system, the pre-satellite period 1958-1972 when no satellite data were available, and the transition period 1973-1988 when the amount of satellite data that were assimilated increases with time. These three periods correspond also to the three streams which were produced separately during the ERA40 production timeframe. The ERA40 dataset is expected to be a major dataset for climate research. Within the ERA40 project, the MPI (Max Planck Institute for Meteorology) had the task to perform a validation of the hydrological cycle. Here, mainly the 6 hour forecasts were considered.

The validation shows that the ERA40 hydrological cycle has changed in several respects compared to the previous ERA15 re-analysis. The hydrological cycle over land is generally improved compared to ERA15. These improvements comprise the eliminated cold biases in winter, the reduced occurrence of negative P-E (precipitation minus evapotranspiration) values, the removed dry bias in winter over Europe, and an improved representation of the snowpack. But the ERA40 hydrological cycle also has several deficiencies. The largest problem is the fact that the global water budget is not only unbalanced, but also P-E over the ocean is positive (and not negative as it should be) in the long term mean for the satellite and transition periods. This is related to an overestimation of precipitation over the ocean, especially in the tropics. The evapotranspiration over land is overestimated for many catchments, and, thus, the corresponding P-E is often underestimated. Using a simplified land surface scheme it was possible to derive improved values of evapotranspiration and runoff from ERA40 precipitation and 2m temperature that are consistent with the ERA40 data. The quality of the hydrological cycle differs between the periods as the biases in the hydrological cycle are strongly influenced by the different observing systems available in the three periods. Therefore, conclusions drawn for hydrological trends should be taken with great care.

1. Introduction

Global numerical weather predictions require initial fields that represent the present state of the atmosphere. These fields are provided by operational analyses and comprise a data assimilation suite combining observations, previous forecasts, and model assumptions about the evolution of different meteorological variables. Since operational analyses are an estimate of the actual weather situation, long time series of these analyses should give an adequate description of the evolution of weather patterns and their statistics would describe the climate.

However, the individual analyses are influenced by changes in the model, in the analysis technique, the data assimilation method and the use of observations. The latter are an essential product of research and development at a numerical weather forecast centre. Thus apparent changes of atmospheric conditions may occur in long time series of analysis fields which are caused only by changes in the corresponding analysis system. This led to the implementation of the re-analysis projects, in which a fixed analysis/forecast system is used to assimilate past observations over a long period of time. (Certain inconsistencies are still present, however, since the amount of available observations and their quality varies for different time periods.) For more detailed information on these topics, see, for example, Uppala (1997) and Kållberg (1997).

The first-generation re-analysis projects have been the fifteen-year re-analysis ERA15 covering the period 1979-1993 produced by the European Centre for Medium-Range Weather Forecasts (ECMWF; Gibson et al., 1997), a fifty-year re-analysis starting from 1948 produced by the National Centers for Environmental Prediction (NCEP; Kalnay et al., 1996), and a fifteen-year re-analysis starting from March 1980 produced by the Data Assimilation Office (DAO) of the National Aeronautics and Space Administration (NASA; Schubert et al., 1995). Although largely successful and widely used, several problems were detected in these first generation re-analyses, such as, e.g., identified for ERA15 by Kållberg (1997) and for ERA15 and NCEP re-analysis including the hydrological cycle over land by Hagemann and Dümenil Gates (2001). For ERA15, these problems, e.g., comprise

- generally too-cold surface air temperatures in winter;
- too-cold spring temperatures in boreal forests;
- unrealistic separation of total runoff into surface runoff and drainage;
- negative precipitation minus evaporation budgets over several catchments;
- the use of unrepresentative data from island stations influencing surface exchanges and precipitation;
- a severe drying of the western Amazonian land surface until corrected half way through the period;
- shifts in temperature and humidity that were subsequently related to problematic assimilation of satellite data (Trenberth et al., 2001).

In order to address these deficiencies and other problems a new 40-year re-analysis (ERA40) has been produced by ECMWF within the EU project ERA-40 for the period from September 1957 to August 2002 (Simmons and Gibson, 2000), which benefits from recent developments of the ECMWF data assimilation system, higher horizontal and vertical resolution and a more comprehensive use of observational data. Due to insufficient observational coverage of many atmospheric variables, researchers in meteorology, climatology, or hydrology often use re-analysis data as pseudo-observations for validation, verification, initialization, or for the forcing of regional models. Therefore the validation by independent data not entered in the assimilation of the re-analysis data itself is an important issue. In the present study we focus on the validation of the hydrological cycle of ERA40, which was an integral part of the EU project ERA-40. General aspects of ERA40 and its validation are described by Uppala et al. (2004).

The importance of the hydrological cycle is highlighted by the Global Energy and Water Cycle Experiment (GEWEX). One of the major GEWEX objectives is the improvement of the ability to simulate both water and energy exchange processes in global climate and weather models. The implications of changes in the hydrological cycle induced by climate change may affect the society more than any other changes, e.g. with regard to flood risks, water availability and water quality. If changes in the hydrological cycle within the last 40 years shall be investigated using the ERA40 dataset its data quality has to be known. Here, one has to identify atmospheric changes and variations introduced into the analyses by changes of availability and of quality of observational data.

Sect. 2 gives some information about ERA40 and on the tools used here to validate the hydrological cycle. Sect. 3 focuses on the global structures of the hydrological cycle and the global water budget in ERA40. Regional studies and results are presented for several large catchments in Sect. 4. In Sect. 5, several fields closely related to the hydrological cycle are considered. Conclusions are given in Sect. 6.

Additional studies of the ERA40 hydrological cycle have been carried out by several authors for specific regions, such as for the French Alpine snow stations (Martin, 2004), for polar regions (Bromwich et al., 2002; Genthon, 2002; Serreze and Etringer, 2002) and for the Mackenzie and Mississippi river basins (Betts et al., 2003a,b). Realistic changes in terrestrial water storage for the Mississippi basin derived from analysed water-vapour fluxes and changes in atmospheric water content are discussed by Seneviratne et al. (2004), while Déry and Wood (2004) use ERA40 data to identify a linkage between the Arctic oscillation and variations in river discharge into the Hudson Bay. Li et al. (2004) report comparisons of soil moisture with data for China, showing generally better results from ERA40 than from NCEP reanalysis or the updated version (Kanamitsu et al., 2002) carried out from 1979 onwards.

2. The ERA40 re-analysis system

The ERA40 model uses a T159 spherical harmonic representation of the atmospheric dynamical and thermodynamical fields, and a grid-point representation of humidity and cloud variables, using a reduced Gaussian grid (Hortal and Simmons, 1991). This grid has an almost uniform distribution of grid points on the sphere, with a grid-spacing of about 110 km. There are 60 levels in the vertical, with a hybrid sigma-pressure coordinate from the surface to 0.1 hPa. The boundary layer and the stratosphere are well-resolved. The ERA40 system uses a recent version of the model physics, including the land-surface scheme described in van den Hurk et al. (2000), and a 3-D variational assimilation system (Courtier et al., 1998) with a 6-hour analysis cycle. Documentation of the Integrated Forecast System (IFS), cycle 23r4, and a summary and discussion of the observations available at different times during the 40-year reanalysis period is available at http://www.ecmwf.int/research/era/ and in Uppala et al. (2004). For simplicity, only full years are considered in the following so that the years 1958-2001 are designated as the ERA40 period. If not mentioned otherwise, all ERA40 data considered in this study were taken from the 6-hour forecasts.

2.1 Additional tools

Particularly for components of the hydrological cycle, such as precipitation data, measurement and representation errors are large (Legates and Wilmott, 1990). In addition, gridded precipitation datasets derived from gauge measurements bear some uncertainties due to different systematic errors (Rudolf and Rubel, 2005), so that the quality of the simulation of the hydrological cycle is difficult to assess. Additional and more precise information can be gained from observed discharges. Therefore it is desirable to use them as additional data to validate the hydrological cycle for large river catchments, since the discharge of most rivers can be measured in principle with comparatively small errors. But as the ERA40 archive does not contain discharge, it has to be derived from the ERA40 data.

In the present study, a hydrological discharge (HD) model (Hagemann and Dümenil, 1998; Hagemann, 1998) is applied to ERA40 to calculate the discharges. It requires time series of daily values of surface runoff and drainage from the soil as input fields. Realistic amounts of these fields are not directly available from ERA40 (see Sect. 5.1). To generate consistent input values, time series of surface runoff and drainage were calculated from the reanalysis data of precipitation and 2 m temperature using a simplified land surface (SL) scheme (Hagemann and Dümenil Gates, 2003). This method to simulate re-analysis discharges using the SL scheme and the HD model has been successfully applied to the previous ERA15 and NCEP re-analyses by Hagemann and Dümenil Gates (2001).

The HD model is a state of the art discharge model that is applied and validated on the global scale. It is also part of the coupled atmosphere-ocean GCM ECHAM5/MPI-OM (Latif et al. 2003). It simulates the lateral freshwater fluxes at the land surface. As a general strategy the HD model computes the discharge at 0.5° resolution using a daily time step. The model input fields of surface runoff and drainage resulting from the various GCM resolutions (such as the ERA40 grid in this study) are therefore interpolated to the 0.5° grid. In the HD model, the lateral water flow is separated into the three flow processes of overland flow, baseflow and riverflow. Overland flow uses surface runoff as input and is representing the fast flow component within a gridbox, baseflow is fed by drainage from the soil and represents the slow flow component, and the inflow from other gridboxes contributes to riverflow. The sum of the three flow processes equals the total outflow from a gridbox. The model parameters are functions of the topography gradient between gridboxes, the slope within a gridbox, the gridbox length, the lake area and the wetland fraction of a particular gridbox.

The SL scheme (Hagemann and Dümenil Gates, 2003) uses daily time series of precipitation and temperature to calculate the main components of the hydrological cycle at the land surface (e.g. soil

moisture, snow accumulation, snowmelt, evapotranspiration, surface runoff, infiltration and drainage). Here, it primarily uses relations which are functions of temperature and precipitation. The time step of the SL scheme is one day, and it uses the same horizontal resolution as the corresponding input data of precipitation and temperature which in the present study are taken from ERA40.

3. Global water budgets and precipitation

The ERA40 time period 1958-2001 can be divided into three parts: the satellite period 1989-2001 (Sect. 3.1), the pre-satellite period 1958-1972 (Sect. 3.3) when no satellite data were available, and the transition period 1973-1988 (Sect. 3.2) when the amount of satellite data increases with time. These three periods correspond also to the three streams which were produced separately during the ERA40 production timeframe. In Sect. 3.4, the ERA40 data are compared to ERA15 for the ERA15 period 1979-1993. Here, also the global precipitation patterns are considered and validated.

With regard to the validation of the ERA40 precipitation over the ocean it has to be mentioned that the precipitation observations over the ocean are very uncertain since almost no direct measurements exists. In the precipitation datasets of HOAPS (Hamburg Ocean-Atmosphere Parameters and fluxes from Satellite data; Graßl et al., 2000), GPCP (Global Precipitation Climatology Project; Huffman et al., 1997) and CMAP (CPC Merged Analysis of Precipitation; Xie and Arkin, 1997), the precipitation values are derived from satellite measurements of infrared and microwave emissions using empirically based algorithms. During this study an error was found in the HOAPS precipitation data before 1992, so that these data should only be used for validation from 1992 onwards. Thus, we have excluded HOAPS data in the following. Currently, version 2 of the HOAPS dataset is being prepared where this error is eliminated (Klepp, MPI, personal communication, 2003).

With regard to the validation of the ERA40 precipitation over land, gridded observational datasets were used that are based on gauge measurements. The datasets comprise CMAP, CRU (Climate Research Unit; New et al., 2000), GPCC (Global Precipitation Climatology Centre; Rudolf et al., 1996) and GPCP data. CRU, CMAP and GPCC data are not corrected for the systematic undercatch of precipitation gauges, which is especially significant for snowfall. For GPCP data, a correction has been applied which is known to be too large by a factor of about 2 (Rudolf and Rubel, 2005) so that the actual precipitation amounts are expected to be in between the corrected and uncorrected data. As only CRU data are available before 1979, we have concentrated on the uncorrected datasets when regional biases are considered in Sect. 4.

3.1 The satellite period 1989-2001

In long term averages (annually or longer), the global water budget should be closed, i.e. the convergence (positive amount of precipitation minus evaporation (P-E)) of moisture over land should equal the divergence (negative P-E) of moisture over the ocean. Table 1 compares the global water budget over land and sea of ERA40 and ERA15 with climatological values of Baumgartner and Reichel (1975; henceforth labelled BR) and precipitation data of GPCC, GPCP and CMAP. The values for ERA40 yield that its global water budget is not closed, and, in addition, there is unrealistic convergence of moisture over the ocean instead of divergence. This moisture convergence over the ocean is even larger than the convergence over land. The latter agrees well with BR. In ERA15, P-E is underestimated over land, but although the total water budget in ERA15 is not closed either, the P-E values over the ocean within this period (1989-93) agree well with BR, as it is also the case for P and E.

The unrealistic moisture convergence over the ocean is closely related to an overestimation of precipitation over the ocean. Figure 1c shows the monthly mean precipitation over the ocean since 1987. For ERA40, the years 1987-1988 are taken from the initialization period of the first ERA40 stream. The ERA40 precipitation

over the ocean shows an unrealistic positive trend which can be seen neither in ERA15 nor in the two observational estimates of GPCP and CMAP. Part of the unrealistically large precipitation values are related to an erroneous bias correction in the assimilation of SSMI (entering the system in September 1987, corrected in the end of 1993) and HIRS data (starting in July 1991, corrected in the end of 1996). The latter was related to the fact that a new NOAA satellite was launched in July 1991. The bias correction was tuned to the present state of the atmosphere which was largely distorted by the aerosols from the Pinatubo eruption at this time. But even after the correction of the HIRS bias correction error which causes a drop of the precipitation over the ocean in January 1997, the precipitation is still too large. It also shows an unrealistic

Table 1. Global water balance over land and ocean for the years 1989-01 in 1015 kg/a. BR designates climatological estimates according to Baumgartner and Reichel (1975). (ERA15: 1989-93, GPCC:1989-2000, CMAP: 1989-99)

Data field at T106	ERA40	ERA15	GPCC	GPCP	CMAP	BR
Precipitation over land	116	114	98	106	99	111
Evaporation over land	76	83	-	-	-	71
Precipitation over ocean	496	390	-	378	390	385
Evaporation over ocean	450	434	-	-	-	424
Total runoff	51	46	-	-	-	40
P-E over land	40	31	-	-	-	40
P-E over ocean	46	-44	-	-	-	-39

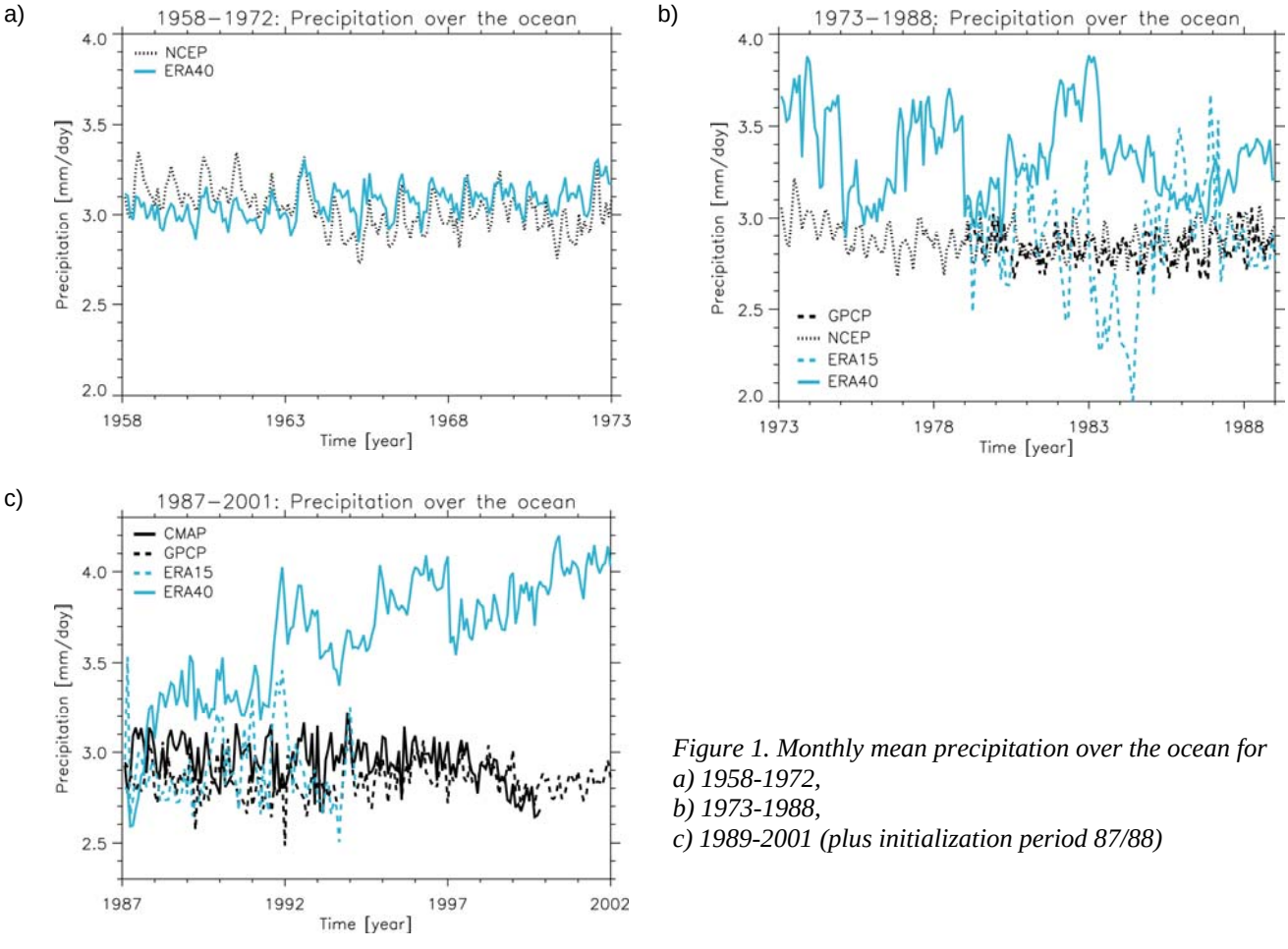

Figure 1. Monthly mean precipitation over the ocean for
a) 1958-1972,
b) 1973-1988,
c) 1989-2001 (plus initialization period 87/88)

increasing trend. The increase in 1998 coincides with the use of radiances from a third HIRS instrument, followed by the use of data from a second SSM/I instrument from 1999 onwards.

Over land, the monthly ERA40 precipitation is much closer to the observations of CMAP and GPCP (Figure 2c) although it seems to be slightly overestimated for most years. Figure 3 shows that the overestimation of precipitation over land and ocean mainly takes place in the tropics. Over the mid- and high northern latitudes the precipitation over the ocean is captured well and lies between the two observational estimates of GPCP and CMAP in the boreal winter (Figure 3a), but it is slightly on the low side in the boreal summer (Figure 3c). This is mainly related to the precipitation over the north-western Atlantic where the ERA40 precipitation is lower than the observational estimates. This is the case for all periods.

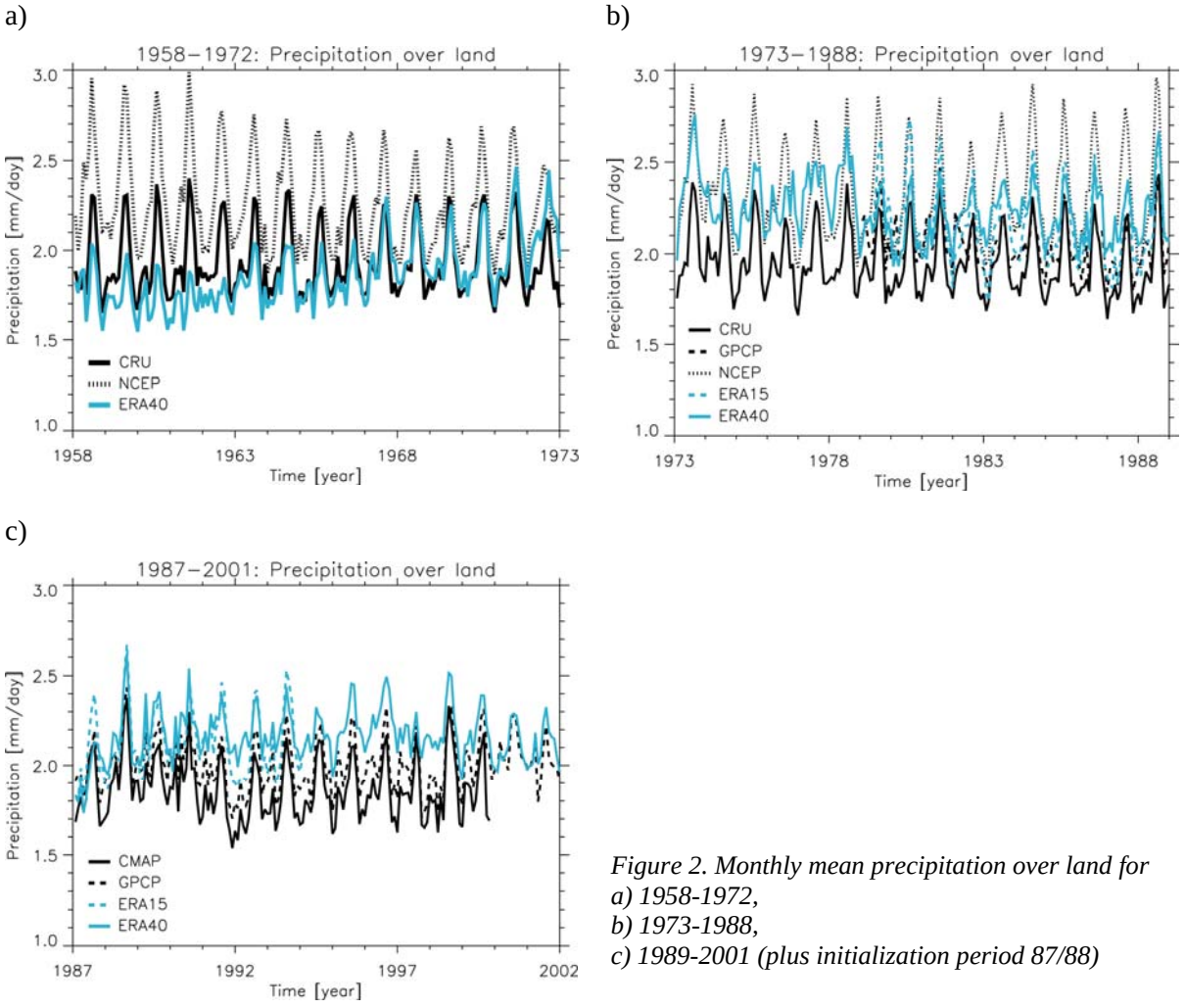

Figure 2. Monthly mean precipitation over land for
a) 1958-1972,
b) 1973-1988,
c) 1989-2001 (plus initialization period 87/88)

Biases in the ERA40 precipitation may be related to the fact that several different observing systems for water vapour are used in ERA40 data assimilation These systems comprise not only the radiosondes (where we know the humidity observations have deficiencies, see, e.g., Zipser and Johnson, 1998) but also HIRS and SSM/I radiances which also have their own problems in using them. Also SYNOP observations are used which may not be representative for the free atmosphere. The variational assimilation tries to adjust the model atmosphere to fit all observations, taking both the model's own error structures and the error structures of the observations into account when combining the different data. Biases in one dataset may be in conflict with other biases in a different dataset. The result is an analysis which is not necessarily in balance with the model's own 'moist climate'.

Andersson et al. (2004) discuss how the ERA-40 analyses were generally moistened over tropical oceans by the assimilation of satellite data. The infrared VTPR and HIRS data were assimilated only in regions judged to be cloud-free, and SSM/I data were assimilated only in regions judged to be rain-free. Forecast estimates (first guess) in these regions were drier than indicated by the data resulting in positive humidity increments. The problem of excessive rainfall resulted in part from the way the humidity analysis spread increments in the horizontal, which not only moistened regions that the data indicated were too dry, but also added moisture in neighbouring regions that were already close to saturation. Rainfall was thus increased where it occurs naturally. In addition a feedback process was suggested, whereby the too-intense tropical circulations driven by latent-heat release produced further drying in the descent regions, which led to further moistening by the data assimilation (see also Uppala et al., 2004).

Note that the precipitation rate from the 24-36h forecasts is generally smaller than from 6h forecasts beyond 1991, but still considerably larger than GPCP and CMAP data (Uppala et al., 2004).

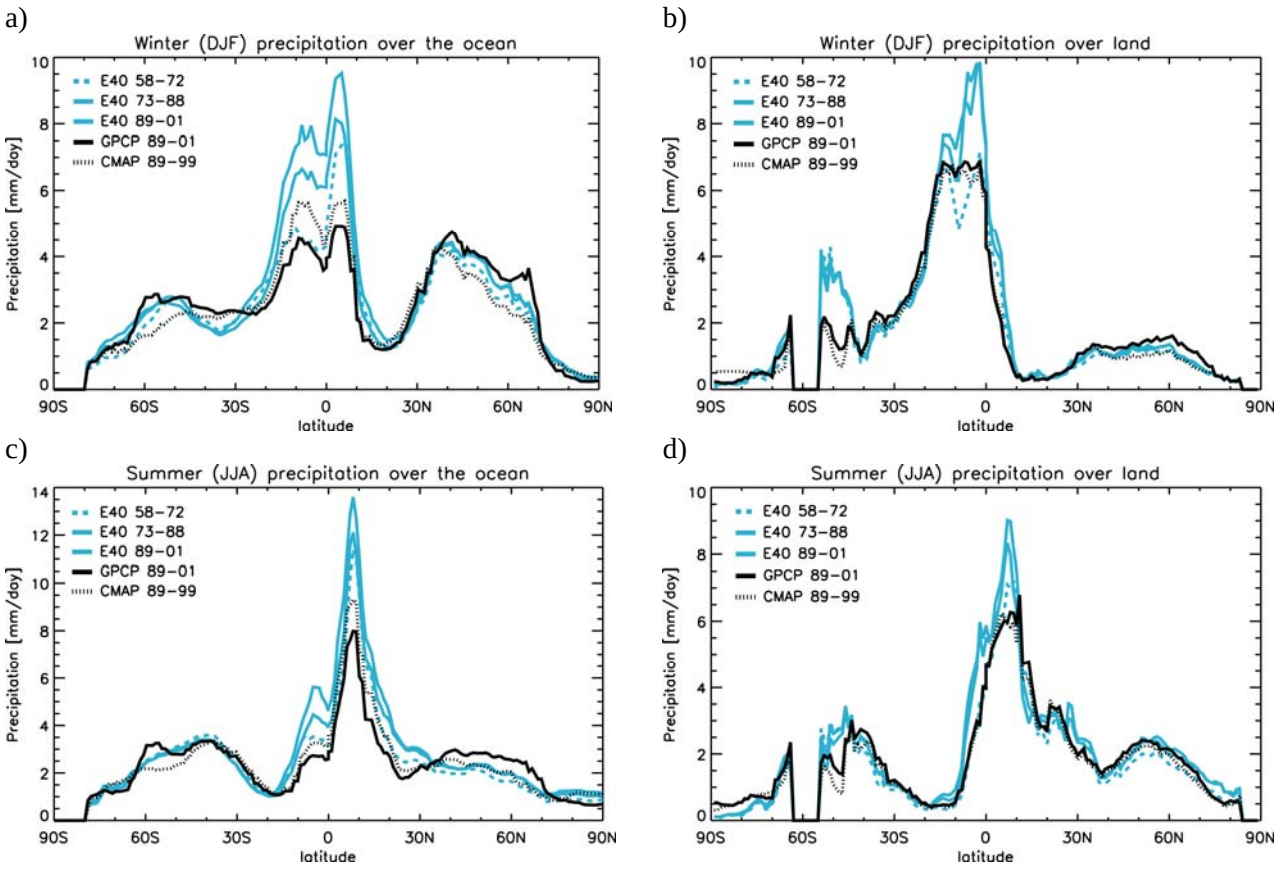

Figure 3. Zonal means of precipitation in the winter over a) the ocean and b) land, and in the summer over c) the ocean and d) land.

3.2 The transition period 1973-1988

For the second period, P-E is slightly negative over the ocean (Table 2) but it is still largely unbalanced compared to P-E over land. As for the satellite period, this seems to be caused by a overestimation of precipitation over the ocean.Figure 1b shows that the monthly mean precipitation in this period is characterized by three peaks where the ERA40 precipitation is much larger than the precipitation estimated by NCEP and GPCP (from 1979-onwards).

Table 2. Global water balance over land and ocean for the years 1973-88 in 1015 kg/a. BR designates climatological estimates according to Baumgartner and Reichel (1975). (ERA15 and GPCP: 1979-88, NCEP at R144 grid)

Data field at T106	ERA40	ERA15	NCEP	GPCP	CRU	BR
Precipitation over land	119	115	115	109	99	111
Evaporation over land	74	80	94	-	-	71
Precipitation over ocean	445	382	376	377	-	385
Evaporation over ocean	453	448	420	-	-	424
Total runoff	55	46	-	-	-	40
P-E over land	45	35	21	-	-	40
P-E over ocean	-8	-66	-44	-	-	-39

Figure 4 shows the anomalies of global precipitation and SST with regard to the time period 1979-98 with the annual cycle removed. For the first and partially also for the third peak and the following decrease it seems that the ERA40 precipitation over the ocean has a strong sensitivity to the SST. But this sensitivity can not be observed for the second peak. It is an open question if this a real sensitivity in the ERA40 system or if the two anomalies curves are only incidentally similar. The NCEP re-analysis does not show any large variations in the precipitation over the ocean at all, and thus the global mean precipitation is not sensitive to the global SST.

Over land, the global precipitation seems to be slightly (Figure 2b) overestimated, especially in the earlier years of the period, which is mainly based on a overestimation of precipitation in the tropics (Figure 3b and Figure 3d). Partially this may be within the uncertainty of the precipitation estimates. For several large catchments this will be investigated more thoroughly in Section 4.

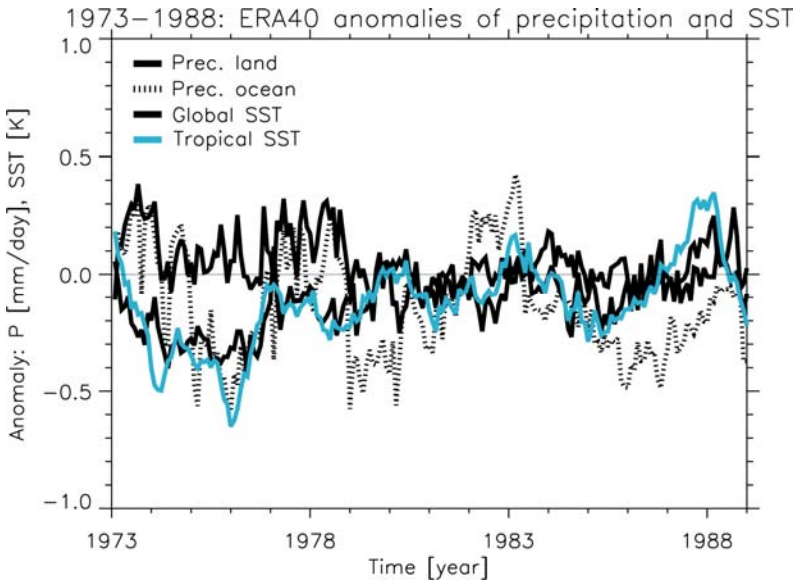

Figure 4. Monthly ERA40 anomalies of precipitation and SST for 1973-1988.

3.3 The pre-satellite period 1958-1972

For the earliest period, P-E over the ocean is negative (Table 3) as it should be. Here, the precipitation over the ocean is largely reduced compared to the other two periods. It even seems to have a small negative bias that is probably related to an overestimation of evapotranspiration over the ocean. This suggestion is

supported by results of (Miller, personal communication, 2001) who found that the simulated boundary layer is too active during this period.

Table 3. Global water balance over land and ocean for the years 1958-72 in 1015 kg/a. BR designates climatological estimates according to Baumgartner and Reichel (1975). NCEP data were made available by NCEP at R144 and T62 grid.

		NCEP			
Data field at T106	ERA40	R144	T62	CRU	BR
Precipitation over land	99	112	120	103	111
Evaporation over land	71	94	-	-	71
Precipitation over ocean	408	395	403	-	385
Evaporation over ocean	465	442	-	-	424
Total runoff	39	-	-	-	40
P-E over land	28	18	-	-	40
P-E over ocean	-57	-47	-	-	-39

In this period, precipitation over land is underestimated which leads to an underestimation of P-E over land. This underestimation is particularly strong over North America where P-E is even negative over a large area (Figure 9a, see Section 3.4.2). Figure 2a shows that the underestimation of global precipitation over land is particularly large in the earlier years until 1966. From 1967 onwards, the ERA40 precipitation over land is very close to the CRU data.

The precipitation over the ocean does not show any large variations in this period (Figure 1a). Due to a lack of observations the ERA40 precipitation over the ocean is compared to NCEP re-analysis (NRA) only. The latter has a similar variability but shows a strange general decrease around 1964. The same applies to the NRA evapotranspiration over the ocean which means that the intensity of the hydrological cycle in NRA is generally reduced from 1964 onwards. It is very unlikely that such a general change in the hydrological cycle occurs very sharply so that something in the NRA assimilation system must have caused this change. A further investigation of this change in NRA is beyond the topic of this study.

3.4 Comparison to ERA15 (1979-1993)

Table 4 compares the global water budgets over land and sea of ERA40 and ERA15 with the observational estimates for the ERA15 period 1979-1993. As for ERA40, the 6-hour forecasts are used for the ERA15 values. Note that ERA15 had a considerable positive spin-up that affected the hydrological cycle over the ocean and the precipitation over land (Stendel and Arpe, 1997). In Table 4, again the overestimation of precipitation over the ocean by ERA40 is shown, which was mentioned before for the two later ERA40 periods in Sect. 3.1 and 3.2. Here, ERA15 is more realistic as its precipitation over the ocean lies between the two observational estimates of GPCP and CMAP. Consequently ERA40 has too low negative P-E values over the ocean, but ERA15 has too largely negative P-E values that point to a probably overestimated evaporation over the ocean.

For ERA40, P-E over land is close to the observational estimate of BR while it is underestimated by ERA15, which points to an overestimation of evaporation over land, too. In some regions, even negative values of P-E over land occur in ERA15. This known bias of ERA15 (e.g. Stendel and Arpe, 1997) and how it has improved in ERA40 is considered in more detail in Sect. 3.4.2.

Table 4. Global water balance over land and ocean for the period 1979-93 in 1015 kg/a (GPCC: 1986-93). BR designates climatological estimates according to Baumgartner and Reichel (1975).

Data field at T106	ERA40	ERA15	GPCC	GPCP	CMAP	BR
Precipitation over land	117	114	98	108	101	111
Evaporation over land	74	81	-	-	-	71
Precipitation over ocean	448	385	-	376	399	385
Evaporation over ocean	455	444	-	-	-	424
Total runoff	52	46	-	-	-	40
P-E over land	42	33	-	-	-	40
P-E over ocean	-7	-59	-	-	-	-39

Figure 5 shows that during the ERA15 period (cf. Sect. 3.1 and 3.2), the ERA40 precipitation is overestimated in the tropics over both land and ocean and in both seasons (winter/summer). While over land this overestimation has not significantly changed compared to ERA15 (Figure 5b and d), it has become worse over the ocean compared to GPCP and CMAP data (Figure 5a and c). As a positive effect we note that the northern winter dry bias over land of ERA15 does not exists in ERA40 (Figure 5b). Also, the boreal summer dry bias over the ocean in the mid-latitudes is largely reduced (Figure 5c). In Sect. 3.4.1, the ERA40 precipitation patterns are compared to ERA15 data and validated in more detail for the ERA15 period.

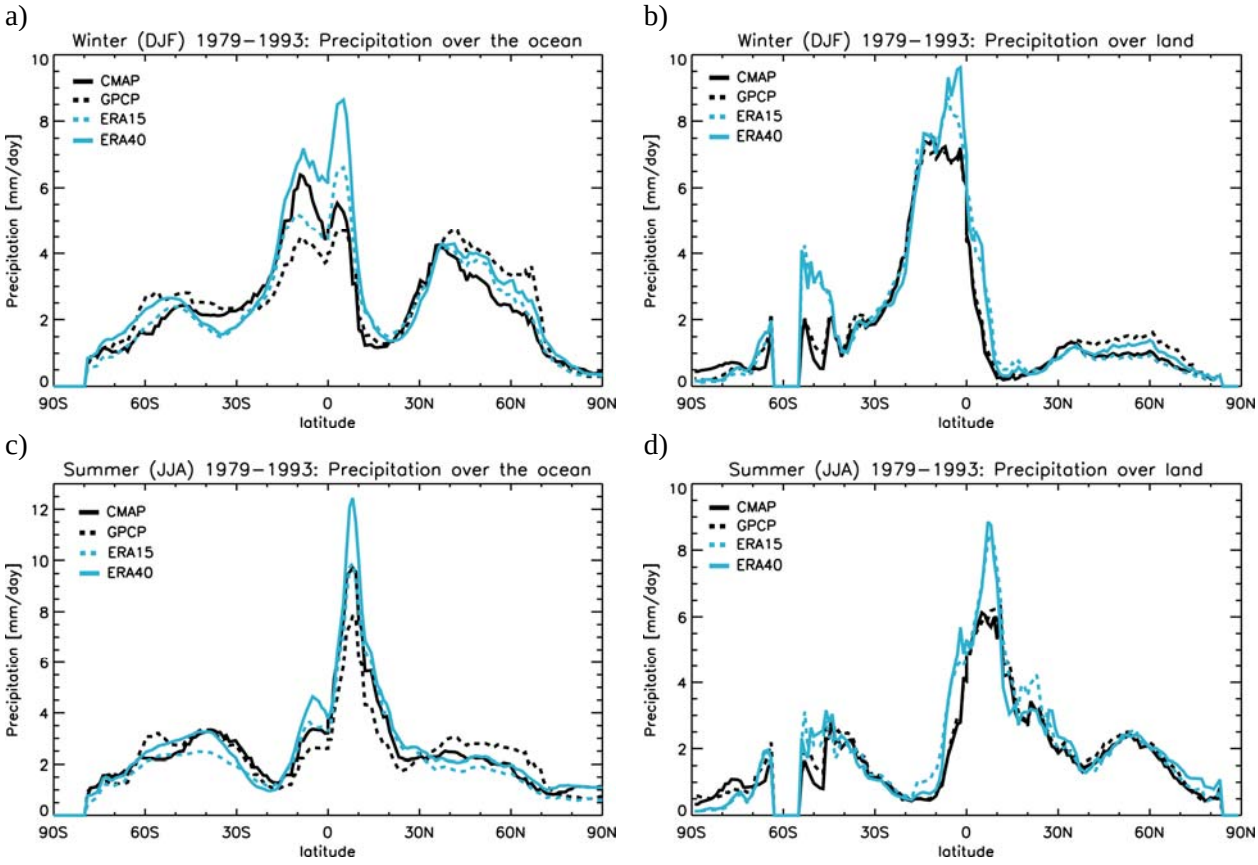

Figure 5. Zonal means of precipitation for the ERA15 period (1979-1993) in the winter over a) the ocean and b) land, and in the summer over c) the ocean and d) land.

3.4.1. Validation of the precipitation patterns for the ERA15 period

In Figure 6, the precipitation differences to GPCP analysis data in the winter (DJF) are shown for ERA15 and ERA40. In the extra tropics, the ERA40 precipitation is generally larger than in ERA15 which seems to be an improvement if compared to GPCP data, especially over the north western Atlantic and Europe where the negative biases in ERA15 are clearly reduced. Earlier studies on operational ECMWF 6h forecasts, where the north western Atlantic dry bias also occurs, have shown that this resulted from too weak convection in the rear of cyclones with cold air outflow from the American continent. The largest differences between ERA40 and ERA15 occur of course in the tropics where there are also the largest amounts of precipitation. ERA40 shows large increases of precipitation over the tropical oceans compared to ERA15, in particular over the tropical Indian ocean and Pacific this increase is exceptionally strong. The comparison with GPCP suggests that this increase is an error. However, there were no geostationary satellite observations available over the Indian ocean which is the most important input for the GPCP analysis over the other tropical oceanic areas and therefore the estimates of GPCP are less reliable for the Indian tropical ocean.

Another area of interest in analyses and model validation has been the SPCZ (South Pacific Convergence Zone). Many models tend to simulate a too strong zonal direction of the SPCZ, more like a double ITCZ. From the difference plots in Figure 6 it is hard to judge if both re-analyses are different in this respect because ERA40 produces much stronger precipitation amounts than ERA15 or GPCP in the tropics and this difference in the amplitudes dominates the difference plots. But plots of the precipitation amounts (not shown) suggest that ERA40 is slightly superior to ERA15 in the positioning of the SPCZ.

Large differences between the different precipitation estimates can be found over tropical South America. However, the uncertainties of the observations in this area are very large and it is hard to judge which of both reanalyses is more realistic although it seems that the biases to GPCP data are slightly reduced in ERA40. The same applies to tropical Africa. The high precipitation amounts along the Andes in both re-analyses are probably erroneous and presumably caused by a numerical problem regarding the representation of orography in the ERA40 model.

During summer (JJA), shown in Figure 7, similarities to the winter season can be found, e.g. much more precipitation in ERA40 in the extra tropics, especially in the winter hemisphere, which seem to be more realistic although the observations are not very reliable in this area. The wet bias over the southern slopes of the Himalaya region is increased in ERA40. We do not know how much precipitation is really falling along the Himalayan mountains where several major Asian rivers have their main sources. The discharge simulations discussed in Sect. 4.2 indicate that the precipitation is indeed overestimated.

The problems over the equatorial South America and Africa as well as over the tropical Indian ocean have already been mentioned above for winter. A new feature is a shift of the Intertropical Convergence Zone (ITCZ) in ERA40 towards the north in the eastern Pacific. Note, e.g., the dipole pattern in the difference plots between ERA40 and GPCP (Figure 7a), which is not present in the ERA15 versus GPCP plot (Figure 7b). In this respect, ERA40 is probably worse than ERA15 as the GPCP data should be able to give a correct position of the ITCZ. The shift of the ITCZ will be discussed in more detail in Sect. 5.5.

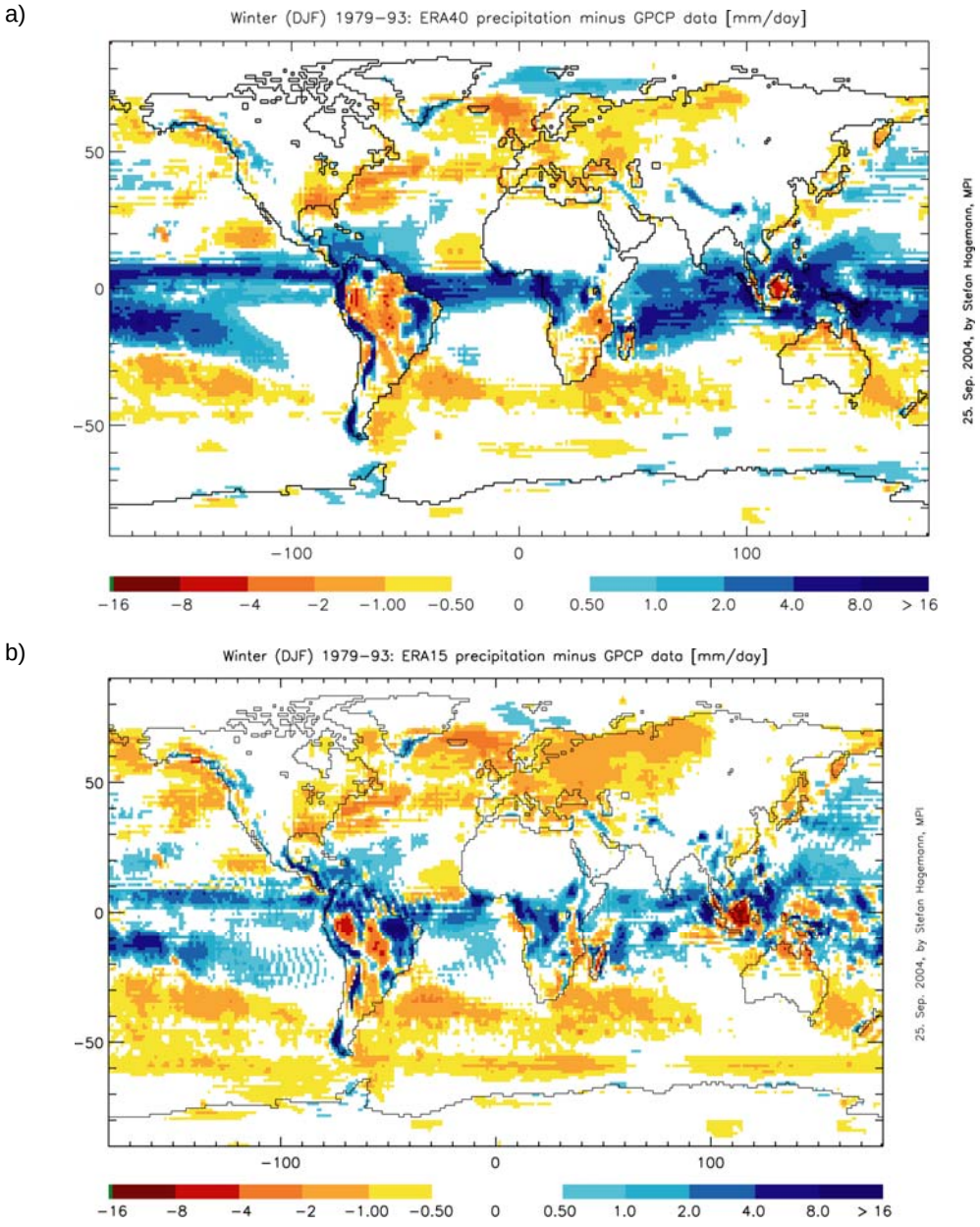

Figure 6. Precipitation difference in the winter (DJF) 1979-93 of a) ERA40 and GPCP data, and b) ERA15 and GPCP data at T106 degree resolution in mm/day.

a)

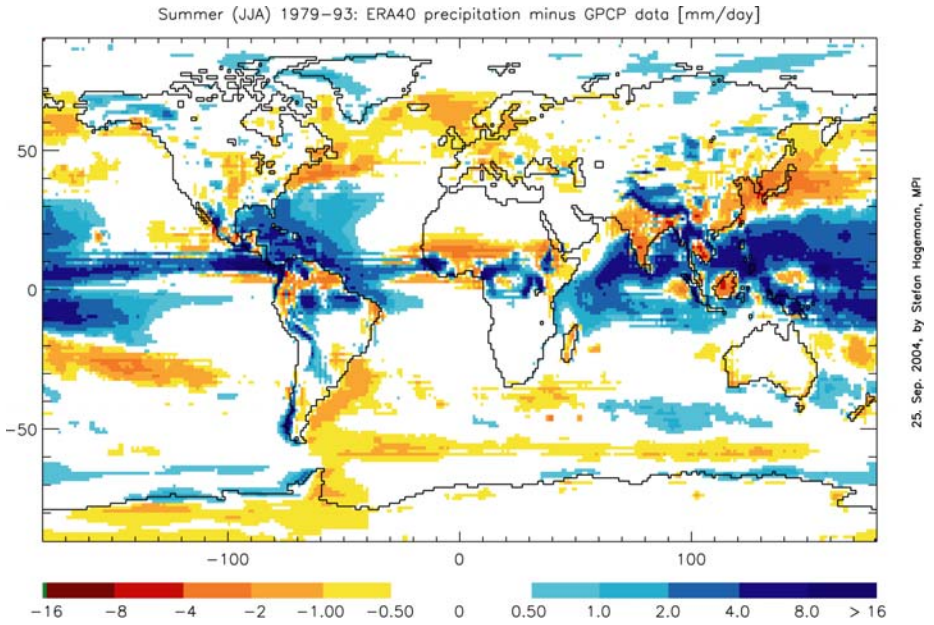

b)

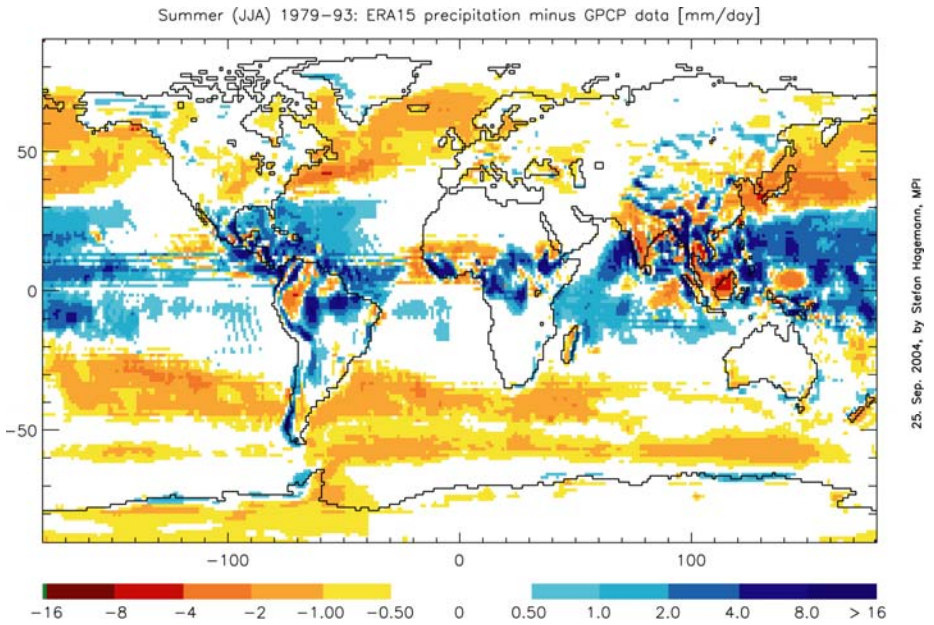

Figure 7. Precipitation difference in the summer (JJA) 1979-93 of a) ERA40 and GPCP data, and b) ERA15 and GPCP data at T106 degree resolution in mm/day.

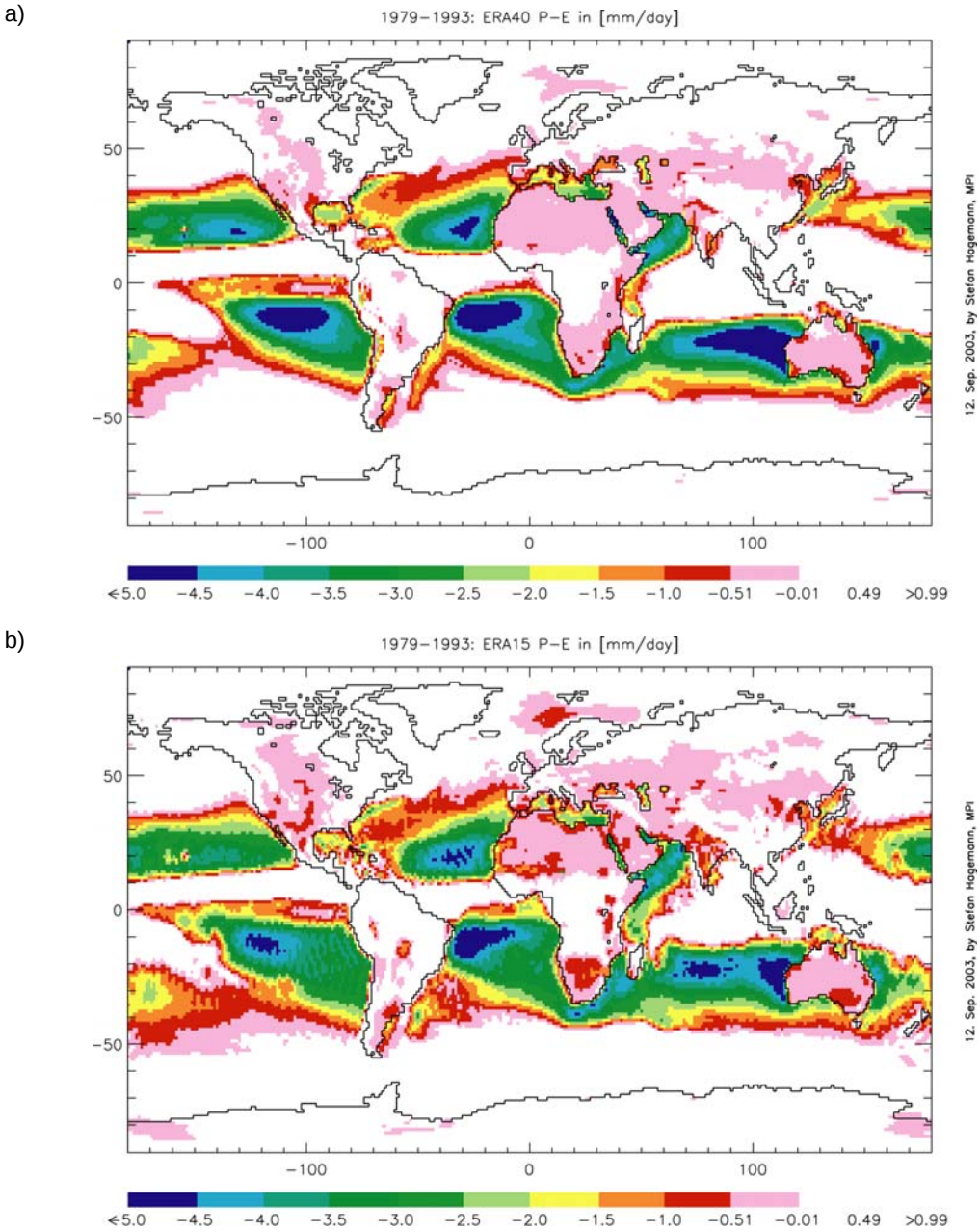

Figure 8. Annual negative P-E of a) ERA40 and b) ERA15 for 1979-1993 in 1 mm/day colour steps.

a)

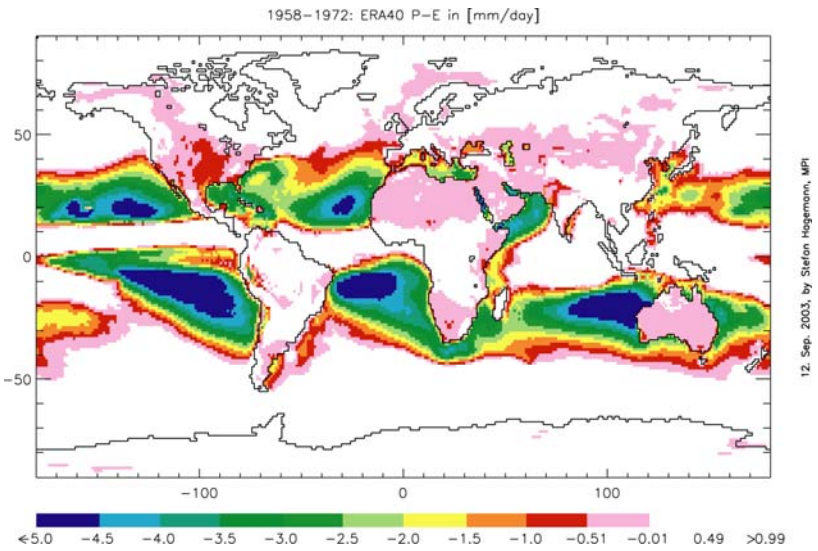

b)

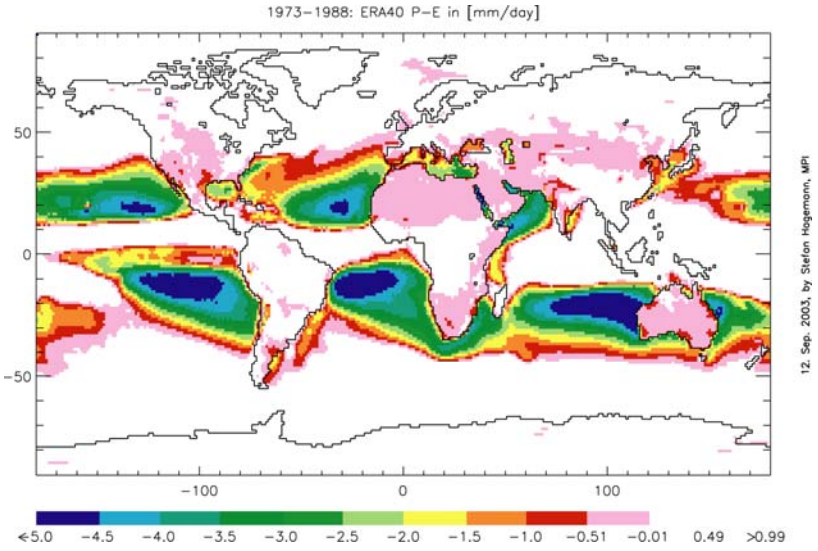

c)

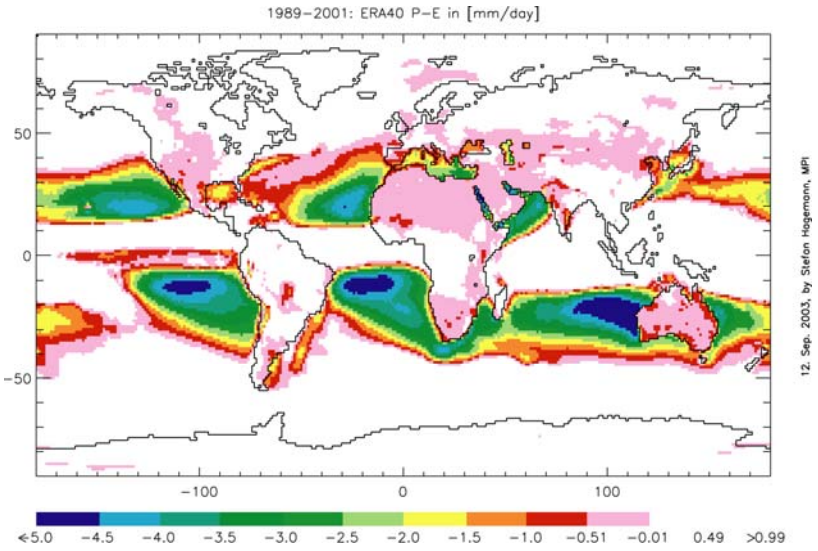

Figure 9. Annual negative P-E of ERA40 for a) 1958-1972, b) 1973-1988, c) 1989-2001 in 1 mm/day color steps.

3.4.2. Negative P-E values over land

Over land P-E should generally be positive. Exceptions are gridboxes in dry areas where sufficient information on re-evaporation of water from rivers enters the ERA40 system via the analysis of screen-level temperature and humidity, e.g. in largely irrigated areas or riverine wetlands (see also Sect. 4.1). Figure 8 shows the mean distribution of negative P-E values for the ERA15 period. The negative annual mean values of P-E over land for ERA15, exceeding at places 0.5 mm/d, are significantly reduced in ERA40 but the bias is still not negligible in a few regions (e.g. North America, Australia, Southern Europe). The latter is the case for all three periods whereas the negative P-E values are most prominent in the pre-satellite period, with especially large values over North America (Figure 9). The annual cycles for the catchments from the corresponding regions (Mississippi, Murray, Danube) show that P-E is negative throughout the year except for the winter months (not shown).

4. Regional studies over large catchments

Figure 10 shows a selection of large catchments for which the ERA40 hydrological cycle is validated in more detail in this section. The catchments comprise the following regions: Amazon, Amur, Arctic Ocean catchment represented by its 6 largest rivers (Yenisey, Kolyma, Lena, Mackenzie, Northern Dvina, Ob), Baltic Sea catchment (land only), Congo, Danube, Ganges/Brahmaputra, Mississippi, Murray, Nile, Parana, Yangtze Kiang. The largest rivers on Earth are included and the catchments were chosen so that they represent various large regions from different climates and continents. In Sect. 4.1, we analyse the regional water budgets of these catchments, and Sect. 4.2 deals with the annual cycles of precipitation and discharge.

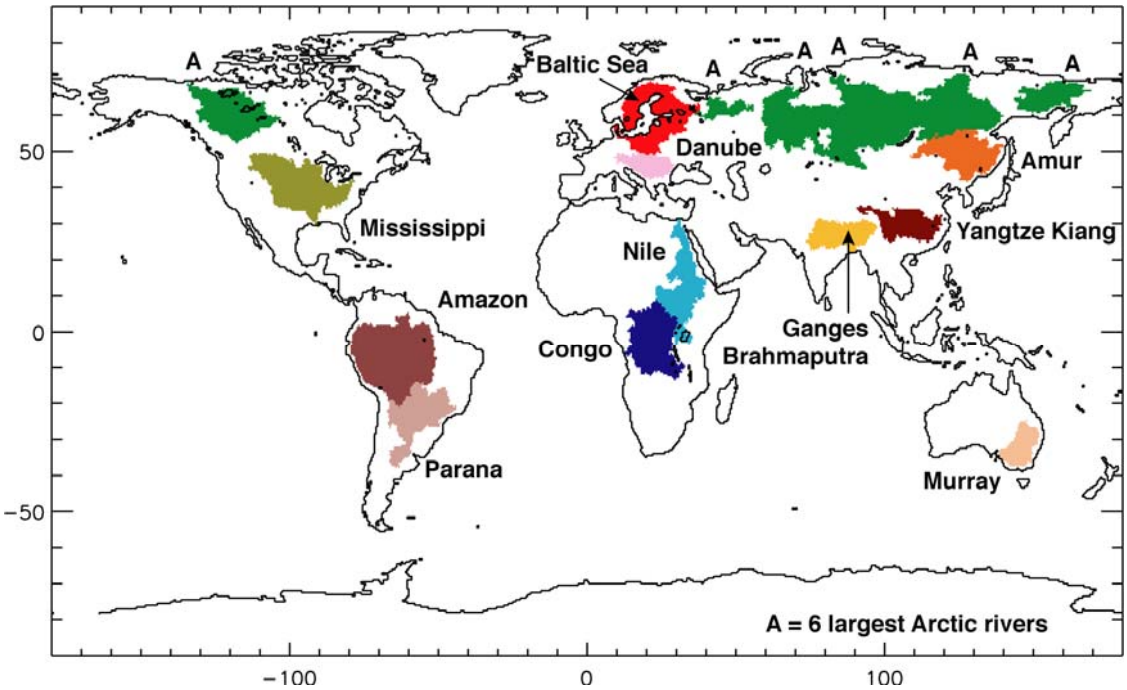

Figure 10. Several large catchments of the globe. The 6 largest Arctic rivers comprise (from west to east) Mackenzie, Northern Dvina, Ob, Yenisey, Lena, Kolyma.

4.1 Regional Water Budgets

Figure 11 shows the precipitation ratio of ERA40 data against observations for all three ERA40 periods. GPCC data are used as observations for the latest period, and CRU data are used for the two other periods. This precipitation ratio gives an idea on the precipitation bias which varies for the 3 periods. For the earliest period, the precipitation ratio is lower than in the two later periods for most of the catchments. For the Nile

river, the ERA40 precipitation is close the observations only in the latest period while it is largely overestimated in the two earlier periods. For Ganges/Brahmaputra it is vice versa. Here, precipitation is largely overestimated only in the latest period (1989-2001).

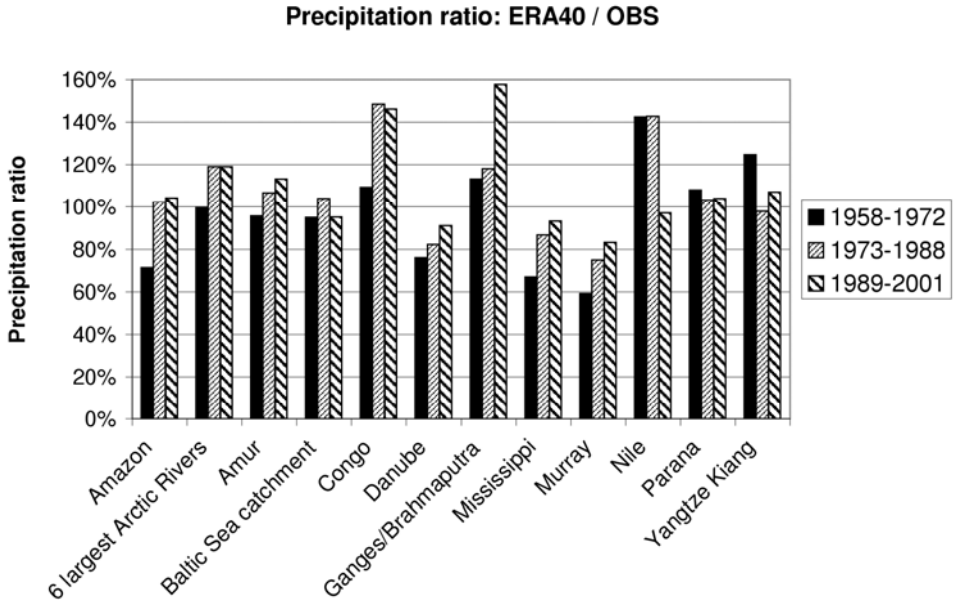

Figure 11. Precipitation ratio of ERA40 to observations for large river catchments. Observations comprise GPCC data for 1989-2001 and CRU data for the two earlier periods.

The fact that the precipitation bias is not the same in all three periods leads to the conclusion that the different observing systems available in the three periods are influencing the quality of the ERA40 precipitation over land. Thus, no conclusions on trends in precipitation over land can be drawn from the ERA40 data. This is supported by Betts et al. (2003b) who found that the bias and spin-up of ERA40 precipitation over the Mackenzie catchment change significantly over the ERA40 period, because of changes in the assimilated data. On an annual basis, both precipitation bias and spin-up are correlated with the analysis increment of atmospheric vertically integrated water vapour. While the different availability of satellite data seems to be primarily responsible for changes in the water vapour after 1972, Betts et al. (2003b) found that changes in the conventional data (or its use) must be responsible in the earliest period.

a) b)

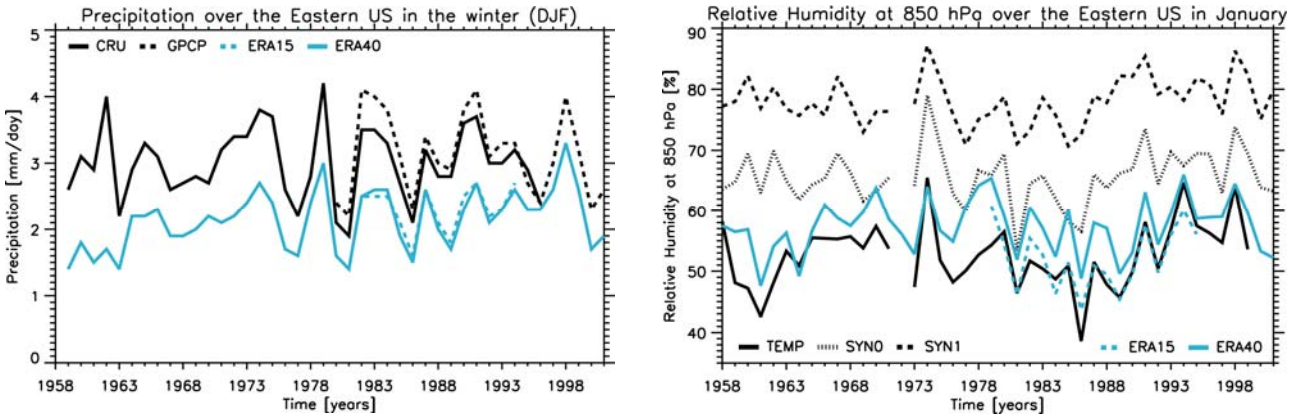

Figure 12 a) Precipitation (DJF) and b) relative humidity at 850 hPa (right panel, January) over the eastern US for 1958-2001 in the boreal winter. TEMP refers to radiosonde measurements over the Eastern US, SYN0 and SYN1 refer to surface observations at 00 GMT and 12 GMT, respectively.

Over the Mississippi catchment, precipitation is underestimated in all three periods with a bias which is systematically decreasing with time. It seems that ERA40 has a general problem to represent the precipitation accurately over the US which was also seen in Figure 6 and Figure 7. This could be related to biases in the humidity observations of North American radiosondes. Figure 12 and Figure 13 show that trends in the precipitation over the eastern US go hand in hand with trends of the relative humidity in the lower troposphere. This is more evident in summer (Figure 13) than in winter (Figure 12). This applies especially to the extreme low values of precipitation and 850 hPa relative humidity up to 1963. The suggestion that biases in the radiosondes lead to too low precipitation values is also supported by a data assimilation experiment (NOHUM) conducted with the ERA40 system by Bengtsson et al. (2004b) where they excluded all humidity data from the assimilation. The experiment was conducted for the summer (JJA) 2000 and the winter (DJF) 2000/2001 and yielded larger precipitation rates than ERA40 over the Mississippi catchment in both seasons: 2.3 (1.7) mm/day compared to 1.8 (1.4) mm/day in the summer (winter).

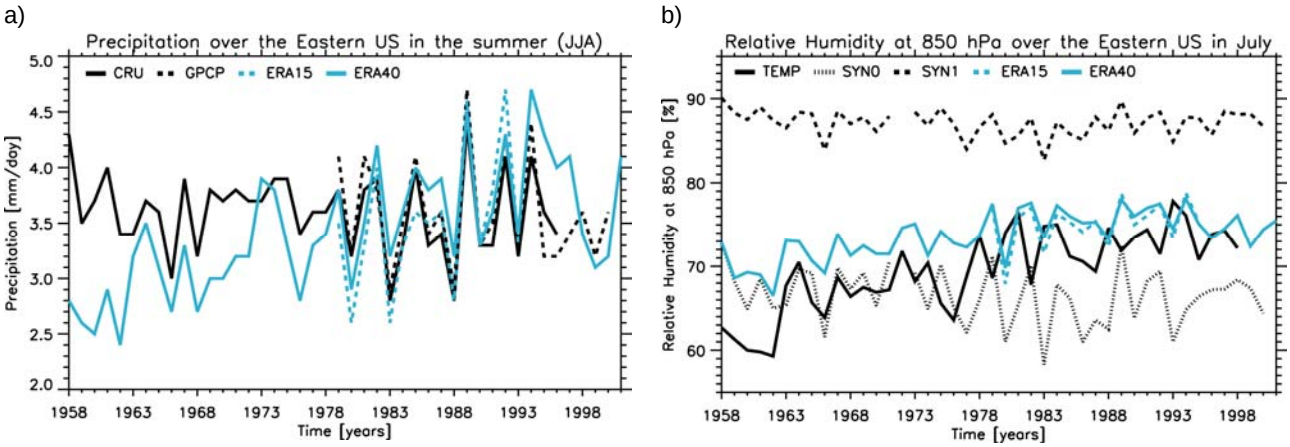

Figure 13 a) Precipitation (left panel, JJA) and b) relative humidity at 850 hPa (right panel, July) over the eastern US for 1958-2001 in the boreal summer. TEMP refers to radiosonde measurements over the Eastern US, SYN0 and SYN1 refer to surface observations at 00 GMT and 12 GMT, respectively.

Figure 14 shows an estimate of the evaporation ratio (ERA40/observational estimate). Here, the actual evaporation was estimated by subtracting the climatological observed discharge (Dümenil Gates et al., 2000) from the observed precipitation. For most of the catchments, evaporation is generally overestimated in ERA40. As for precipitation, the bias varies between the three periods for some of the catchments. Here, the evaporation ratio in the latest period tends to be larger than in the two earlier periods. Comparing the three periods an expected tendency can be seen in the ERA40 data that more precipitation leads to more evaporation over most catchments. Over the Nile catchment, the evaporation is underestimated (Here, observed discharge data were only considered until 1963 to exclude the effect of the Assuan dam). In this region, a lot of irrigation takes place where the water is taken from the Nile river and evaporates over the irrigated areas. As no direct information on irrigation enters the ERA40 system, these high amounts of evaporation cannot be simulated.

However, such information might enter the ERA40 system indirectly, due to the adjustments of soil moisture derived from the analysis of screen-level temperature and humidity if sufficient observations are available in a certain area. The latter is very unlikely for the Nile catchment. In general, adjustments of soil moisture are probably not able to represent the full effect of evaporation from open water (by irrigation) over the ground, which is usually evaporating at the potential rate in irrigated areas, although the adjustments may cause the simulated evaporation to become somewhat larger. Thus, it is very unlikely that the irrigation effect can be simulated for the majority of irrigated land areas.

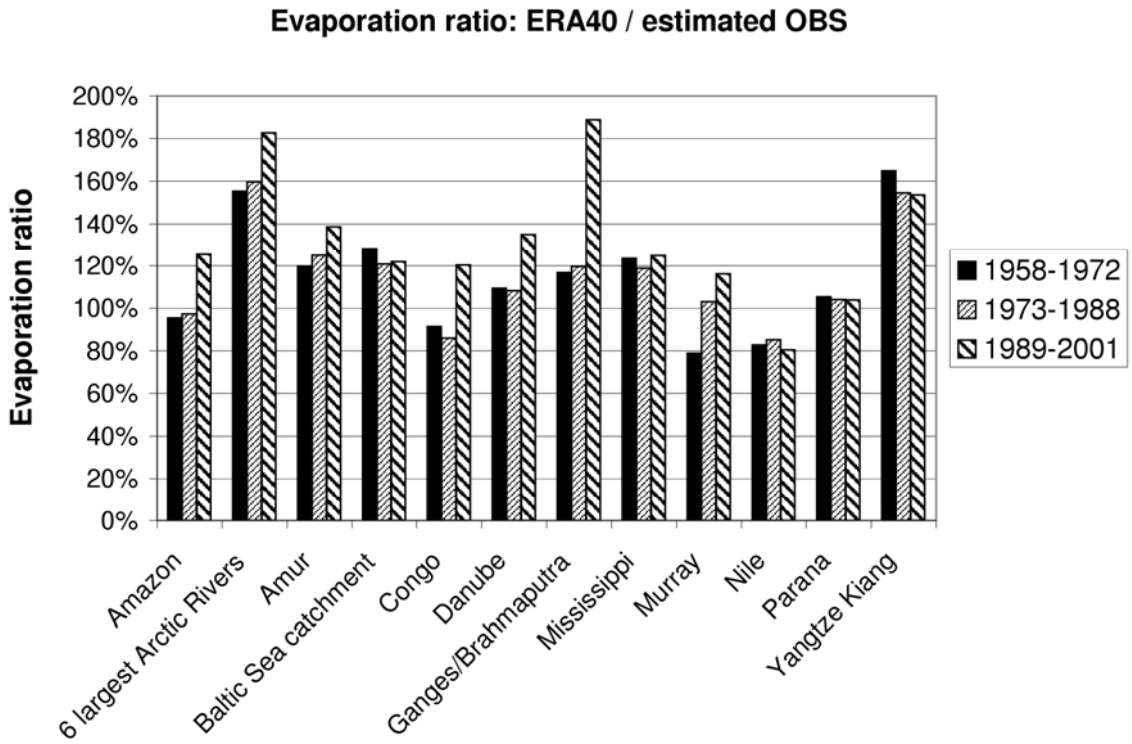

Figure 14. Evaporation ratio of ERA40 to estimated observations for large river catchments. The observed evaporation is estimated from the observed precipitation minus the climatological discharge.

In Figure 15, the runoff ratio is shown, calculated as the ERA40 P-E divided by the climatological discharge. Generally the runoff is underestimated which is mainly related to the too large evaporation. For the Nile, there is a large overestimation of runoff due to the large underestimation of evaporation (see above). For the Congo and Ganges/Brahmaputra rivers, there is partially an overestimation of runoff due to too large precipitation amounts. For the Mississippi, the runoff is negative in all 3 periods which is directly related to the underestimation of precipitation. As discussed in Sect. 3.4.2, this also shows that the water balance is not closed at the land surface due to the soil moisture nudging which acts as a source of water in the Mississippi catchment. Figure 16 shows the bias of the runoff coefficient (runoff divided by precipitation) which clearly illustrates the deficits in the ERA40 runoff (P-E) for most of the catchments.

As the ERA40 hydrological cycle should be additionally validated with observed discharges (see Sect. 2.1), the SL scheme was applied to ERA40 data to calculate daily fields of surface runoff and drainage that are consistent with the ERA40 precipitation and 2m temperature. As a positive side effect, evaporation values were simulated that agree better with the observational estimates than the ERA40 data. This is demonstrated by Figure 17 where the SL scheme evaporation ratio is shown for the three periods. Consequently the SL scheme bias of the runoff coefficient (Figure 18) is much smaller than the ERA40 bias for most of the catchments. Thus, the SL scheme fields of evaporation and runoff may be used to replace the corresponding ERA40 fields in future studies that require daily fields of the ERA40 hydrological cycle.

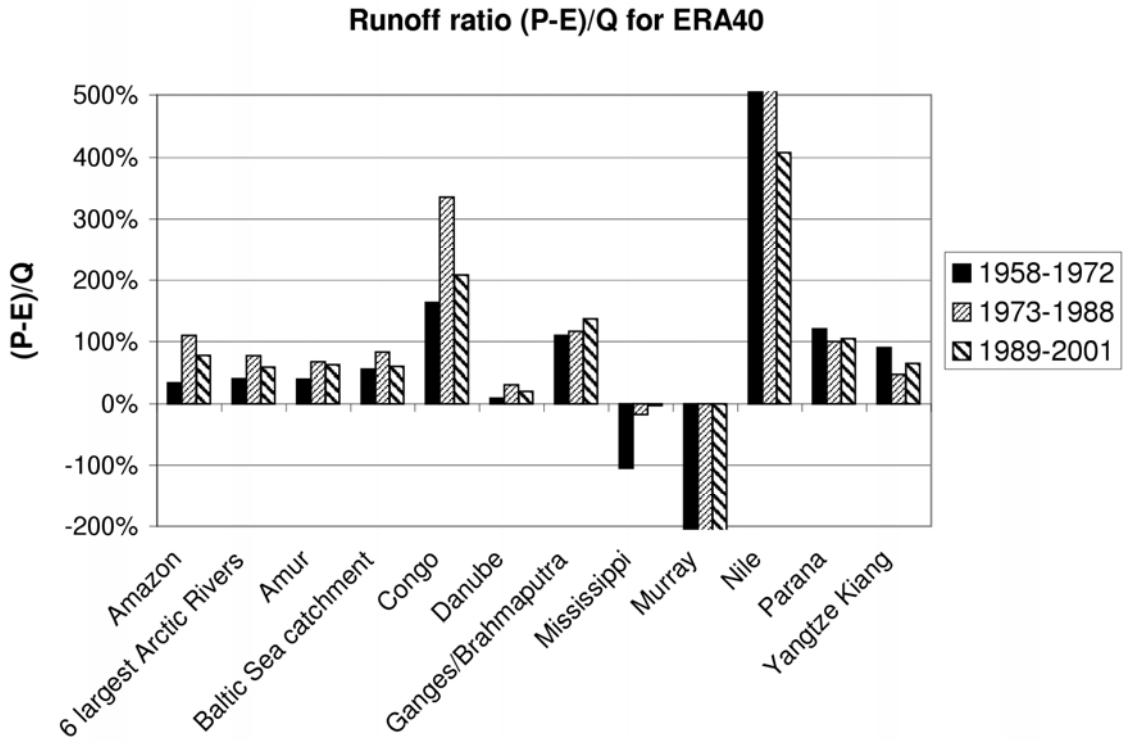

Figure 15. Runoff ratio of ERA40 to observed climatological discharges for large river catchments.

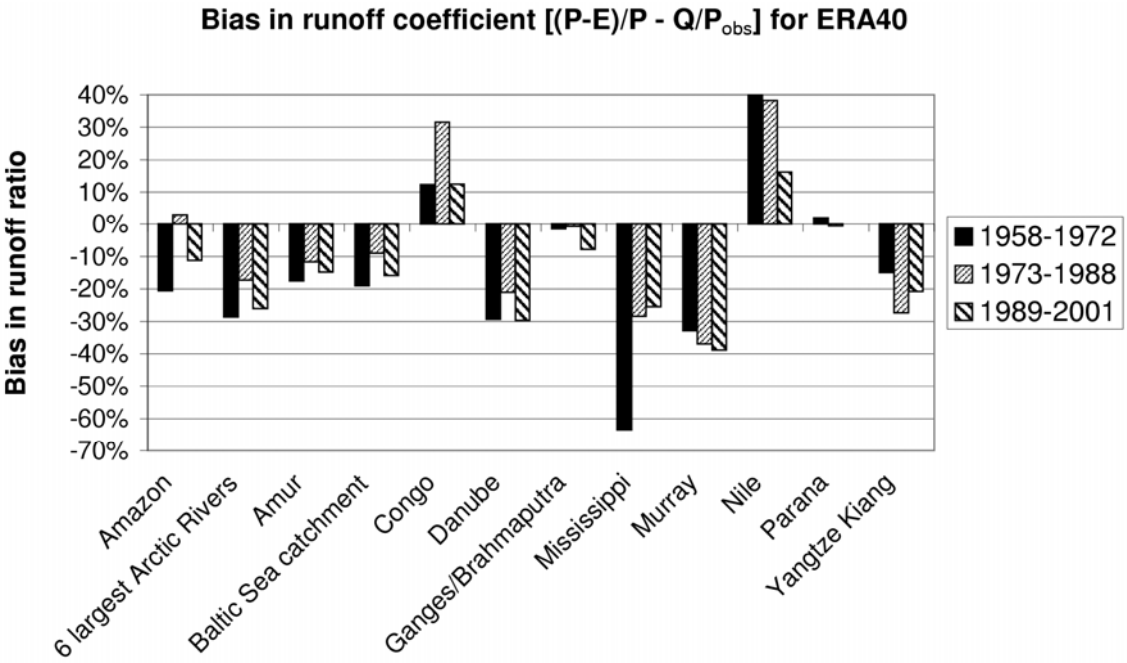

Figure 16. Bias in runoff coefficient (runoff divided by precipitation) of ERA40 for large river catchments.

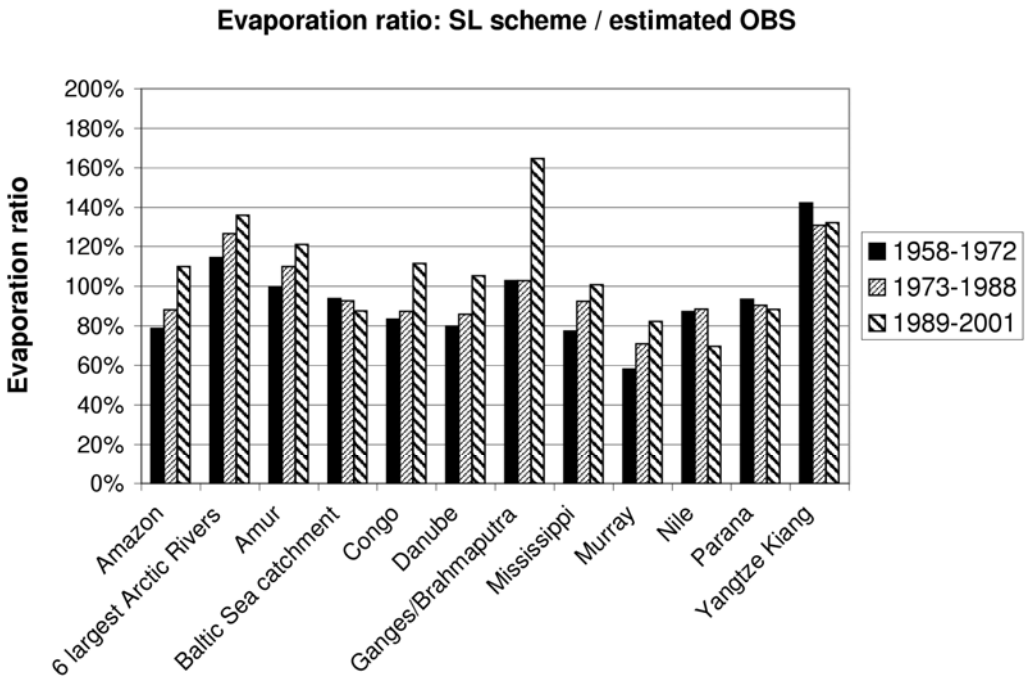

Figure 17. Evaporation ratio of ERA40-SL to estimated observations for large river catchments. The observed evaporation is estimated from the observed precipitation minus the climatological discharge.

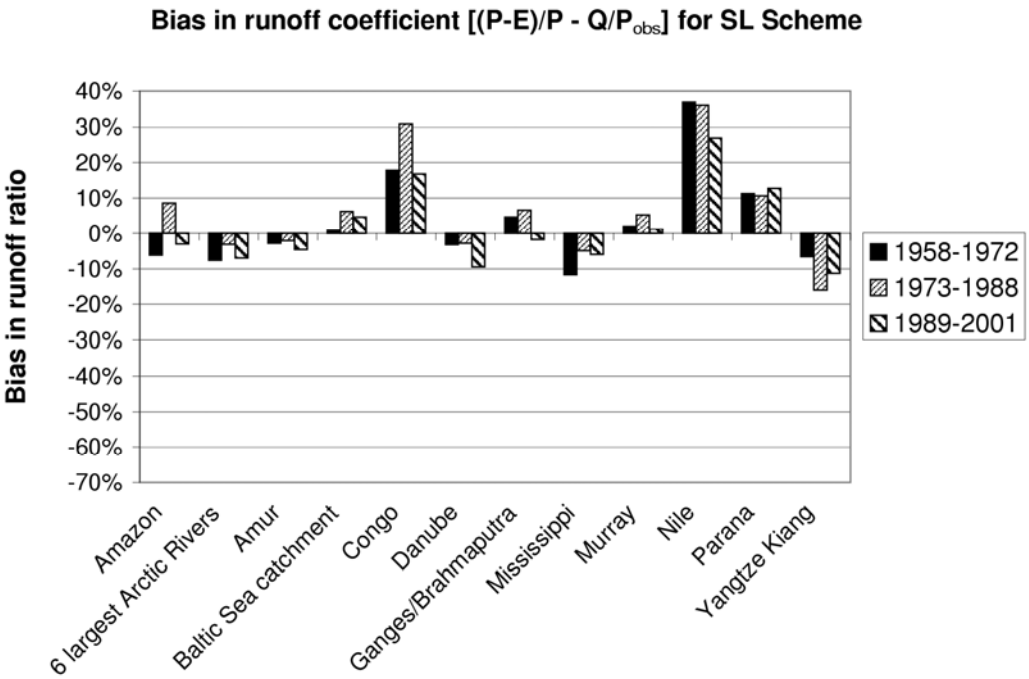

Figure 18. Bias in runoff coefficient (runoff divided by precipitation) of ERA40-SL for large river catchments.

4.2 Annual Cycles

Figure 19 shows the monthly mean annual cycles of precipitation for several selected catchments. It can be seen that regional biases in the annual precipitation (Figure 11) are connected to different biases in the seasonal cycle of precipitation.

For the Arctic Ocean catchment represented by its six largest rivers (Figure 19a), the annual cycle of precipitation lies well within the two observational datasets of GPCC and GPCP. Exceptions arise in the boreal summer when a low precipitation bias occurs in the earliest period and a wet bias in the intermediate period.

A low precipitation bias in the boreal summer also comes up over the maritime climate of the Baltic Sea catchment (Figure 19a) for all periods, which is strongest in the earliest period. Over the more continental climate of the Danube catchment (Figure 19a), a general dry bias is shown in all periods. Here, the largest dry bias occurring in the late summer/early autumn looks similar to the so-called summer drying problem, which is a problem that many GCMs and particularly regional climate models have (e.g. Hagemann et al., 2004). But for ERA40, the dry bias is most likely related to the assimilation of atmospheric humidity data as the precipitation is largely increased in the NOHUM experiment (cf. Sect. 4.1), especially in the summer. The NOHUM experiment yielded 2.4 (1.5) mm/day compared to 1.4 (1.3) mm/day in the summer (winter) 2000. In addition, the long term variability of annual precipitation over the lower Danube catchment (not shown) is similar to the variability of the 850 hPa relative humidity of radiosonde observations in this area.

Over the Indian monsoon region represented by the Ganges/Brahmaputra catchment (Figure 19b), the wet bias in spring suggests that the onset of the ERA40 monsoon precipitation happens too early within the year in all periods. Over the east Asian monsoon region represented by the Amur and Yangtze Kiang catchments (Figure 19b), the timing of the monsoon precipitation generally agrees well with the observations except in the earliest period over the Yangtze Kiang catchment where the decrease of the monsoon precipitation in the autumn occurs about one month too late. In this catchment, a dry bias in the intermediate period is confined to the most intense part of the monsoon during the boreal summer.

Over the two African catchments (Figure 19c), a general wet bias shows up. For the Congo, this wet bias occurs in all periods and it is smallest in the boreal summer and in the earliest period. For the Nile, the wet bias only shows up in the two earlier periods and is strongest in the boreal summer.

Similarly to the Danube catchment, a general dry bias shows up over the Australian Murray catchment (Figure 19c) in all periods. This dry bias is strongest in the earliest period and less severe in the latest period. But contrary to the Danube catchment, the assimilation of humidity data does not seem to cause this bias as no increase of precipitation is yielded in the NOHUM experiment.

Figure 19d shows that the large underestimation of precipitation over the Mississippi catchment in the earliest period (cf. Figure 11) is connected to a dry bias extending over the whole year. The smaller dry bias in the intermediate period is mainly confined to the boreal summer, although the ERA40 precipitation in the two later periods is generally more on the low side as it is close to the uncorrected GPCC data (cf. Sect. 3).

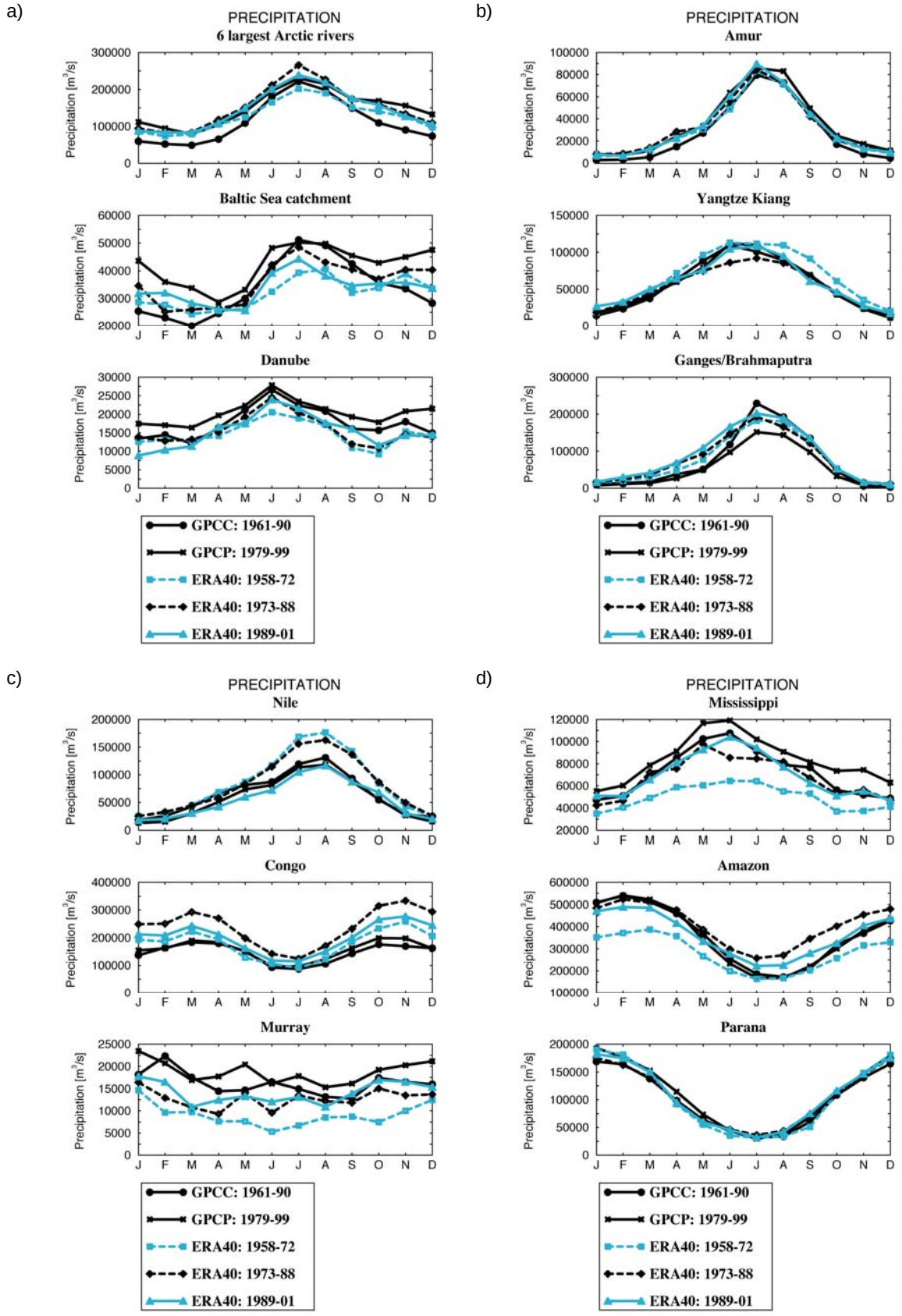

Figure 19. Precipitation over selected catchments in a) Arctic Ocean catchment and Europe, b) Asia, c) Africa and Australia, d) North and South America

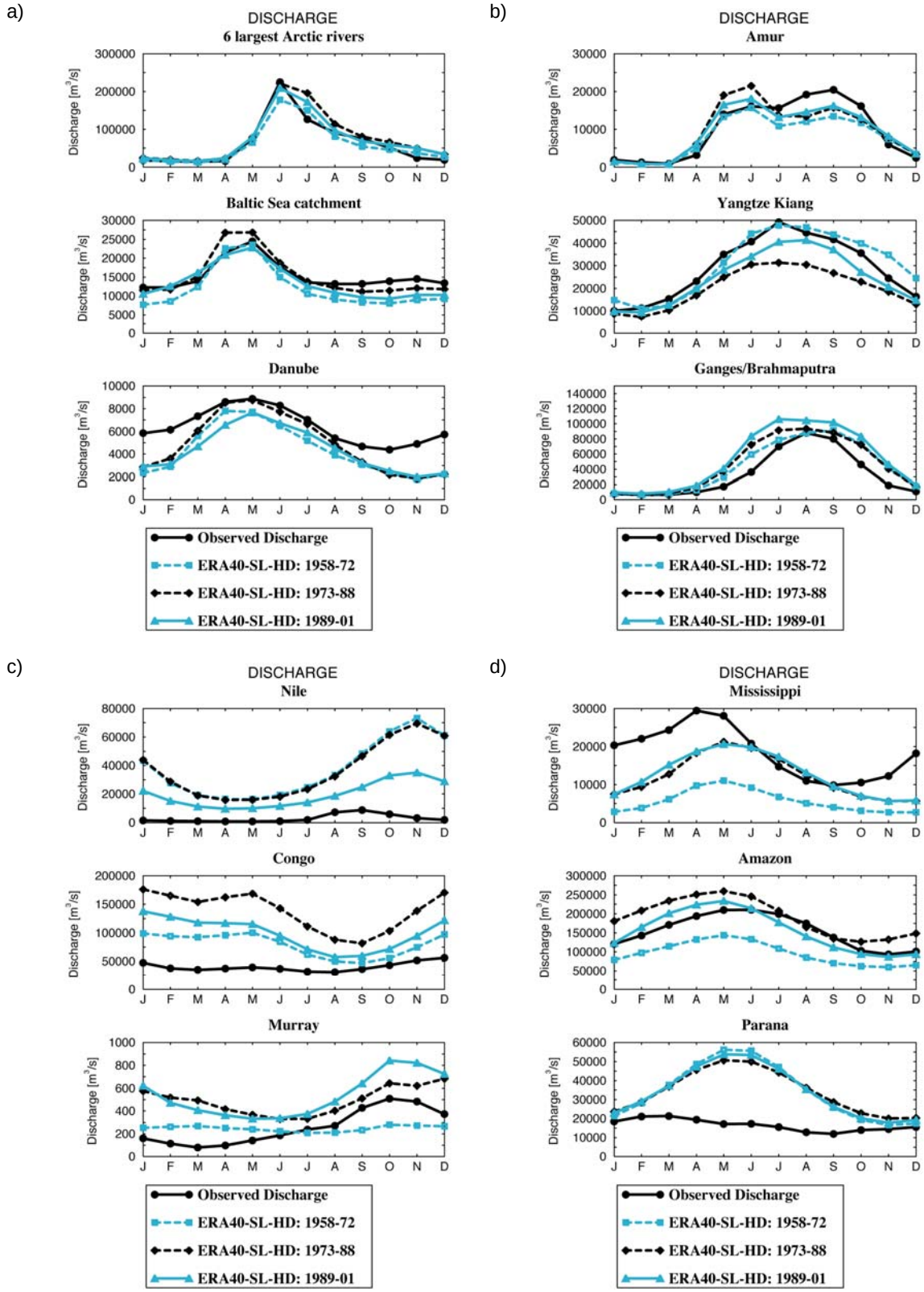

Figure 20. Discharge simulated with SL scheme and HD model for selected catchments in a) Arctic Ocean catchment and Europe, b) Asia, c) Africa and Australia, d) North and South America

The characteristics of the ERA40 precipitation over the two South-American catchments differ largely. While over the Parana catchment (Figure 19d) the ERA40 precipitation agrees well with the observations in all periods, its accuracy is significantly different in the three periods over the Amazon catchment (Figure 19d). The dry bias in the earliest period (see above) is opposed by wet biases occurring in the boreal summer of the latest period and in the second part of the year of the intermediate period. These differences are not primarily caused by decadal variability as CRU data show variations of less than +/- 2% between the periods while ERA40 shows variations of about +/-12%.

As precipitation observations have some uncertainties related to systematic biases, such as the precipitation undercatch by the rain gauges mentioned in Sect. 3, we also analyse the discharge simulated with the SL scheme and the HD model (Figure 20). In general, the deviations of the simulated discharge from the observed discharge for the different periods are rather consistent to the deviations of the ERA40 precipitation from GPCC and GPCP data.

This suggests that biases in the precipitation of ERA40 are genuine, and not an artefact of problems with precipitation measurements. It also indicates that the SL scheme adequately simulates the monthly mean behaviour of land surface processes for most of the regions. Exceptions are the results for Nile, Murray and Parana.

The large evaporation amounts induced by irrigation in the Nile catchment (cf. Sect. 4.1) can be simulated neither by the SL scheme nor by the HD model as no information on irrigation is entering the model formulations. Therefore the simulated discharge (Figure 20c) is overestimated also for the latest period where the ERA40 precipitation (Figure 19c) is slightly lower than the observations.

For the Murray catchment, the simulated discharges (Figure 20c) are larger than the observed discharge although the ERA40 precipitation (Figure 19c) is lower than the observations in all periods. But given the small amounts of discharge in this very arid region, the deviations are within the uncertainty limitations of model calculations. The total amount of runoff/discharge is only a small fraction of the precipitation (a few percent) so that small deviations in the simulated SL scheme evapotranspiration may lead to larger deviations in the simulated discharge. Here, it is not sufficient to consider only the bias in runoff, but also a measure should be taken into account that pays regard to these uncertainty limitations. In this case, the bias of the runoff coefficient is appropriate (Figure 18), which reveals that the error made in the runoff is very small for the Murray catchment.

For the Parana catchment, the simulated discharge (Figure 20d) is largely overestimated in the southern winter half year although the ERA40 precipitation (Figure 19d) is close to the observations. This is related to the underestimation of evaporation by the SL scheme of about 10%. It seems that certain local features generating high evaporation rates within the Parana catchment, such as the swamps of Pantanal, the Iguacú water falls and the wetlands spread around the whole southern part of the Parana catchment, are insufficiently represented.

With regard to the uncertainty of precipitation biases over the Himalaya region mentioned in Sect. 3.4.1, the Ganges/Brahmaputra catchment is considered where a major part of the catchment is located along the Himalaya mountains. Both the precipitation (Figure 19b) and simulated discharge (Figure 20b) curves indicate an overestimation of spring and summer precipitation, especially during the two later periods.

5. Other fields related to the hydrological cycle

In this section, several ERA40 fields closely related to the hydrological cycle are considered. These fields comprise surface runoff and drainage (Sect. 5.1), 2m temperature (Sect. 5.2), accumulated snowpack (Sect. 5.3) and vertically integrated water vapour (Sect. 5.4). In addition, Sect. 5.5 deals with the precipitation variability in the Tropics.

5.1 Surface runoff and drainage

Similarly to ERA15 (Hagemann and Dümenil Gates, 2001), the separation of the total runoff into surface runoff and drainage is not well represented in ERA40. In many parts of the world the observed surface runoff is larger than the drainage (Gottschalk and Xu, personal communication, 1995). There are some limited regions in Africa where the observed drainage is larger than the surface runoff. An example would be the Senegal catchment where the observed groundwater flow, which is fed by drainage, is twice as large as the surface runoff (Kattan et al., 1987). However, the ERA40 drainage from the soil (at 3 m depth) is larger than its surface runoff by 2 orders of magnitude at the majority of the land points. This is unrealistic for most parts of the world so that it has not been explicitly considered in the present study. Compared to ERA15, the ERA40 surface runoff has improved during the snowmelt season (Viterbo, personal communication, 2001).

5.2 2m temperature

In Figure 21, the 2m temperature of ERA40 and ERA15 are compared to CRU2 (Climate Research Unit Vs. 2) data (New et al., 2002) for the boreal winter (DJF) 1979-93. In ERA40, the large northern hemisphere winter cold bias of ERA15 is replaced by a warm bias over northern Asia and North America. An indication of this warm bias can be already seen in ERA15 in the northern eurasian coastal regions. Therefore it is suggested that the bias is also included in the ERA15 data but it is overlaid by the severe cold bias. For the southern hemisphere, the winter (= boreal summer) cold bias of ERA15 is eliminated in ERA40 (Figure 22). The elimination of the cold bias is mainly related to the inclusion of soil water freezing (Viterbo et al., 1999) and a change in the snow albedo over forest-covered areas (Viterbo and Betts, 1999).

Figure 23 shows the mean monthly cycle of the difference of the ERA40 2m temperature to CRU2 data over selected catchments for the three periods. The warm bias in the winter (see above) over high northern latitudes shows up over the 6 largest Arctic rivers, the Baltic Sea (Figure 23a) and the Amur catchment (Figure 23b). For these catchments, there is an improvement of the temperature bias from the earliest to the latest period. An analogous improvement is also seen for the cold biases over the Nile and Congo catchments (Figure 23c) as well as for the warm bias over the Murray catchment (Figure 23c). Mostly the variation of the temperature bias between the three periods is relatively small, especially if the ERA40 2m temperature is close to the CRU2 data, such as for the Danube (Figure 23a) and the Yangtze Kiang (Figure 23b), or if the bias does not largely vary seasonally, such as for the Ganges/Brahmaputra (Figure 23c) and the Mississippi (Figure 23d). An exception from the latter is the Amazon catchment where the ERA40 2m temperature agrees well with the CRU2 data in the earliest period, but there is an almost constant cold bias of about 1 K in the two later periods.

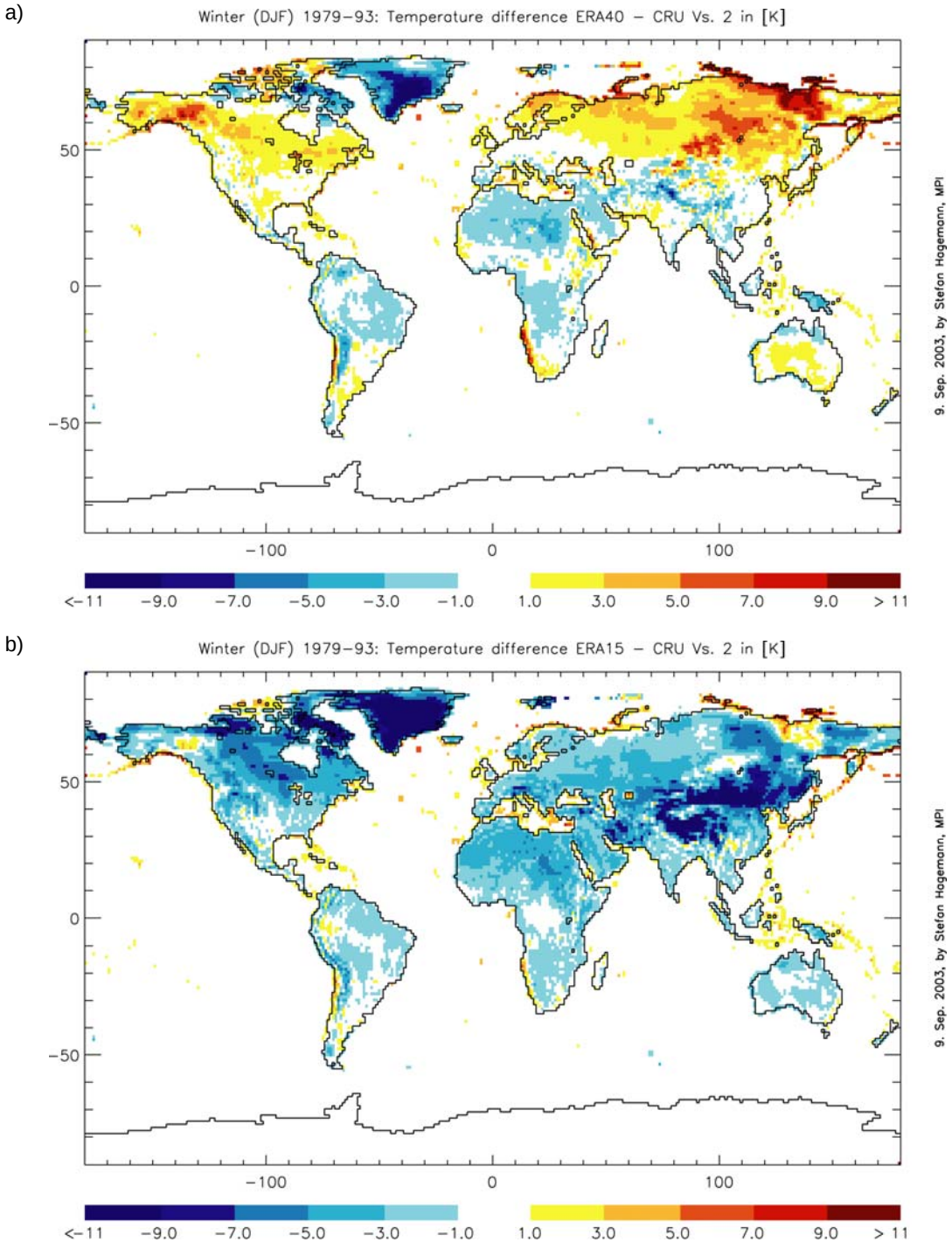

Figure 21. 2m temperature difference in the winter (DJF) 1979-93 of a) ERA40 and CRU2 data, and b) ERA15 and CRU2 data at T106 degree resolution in K.

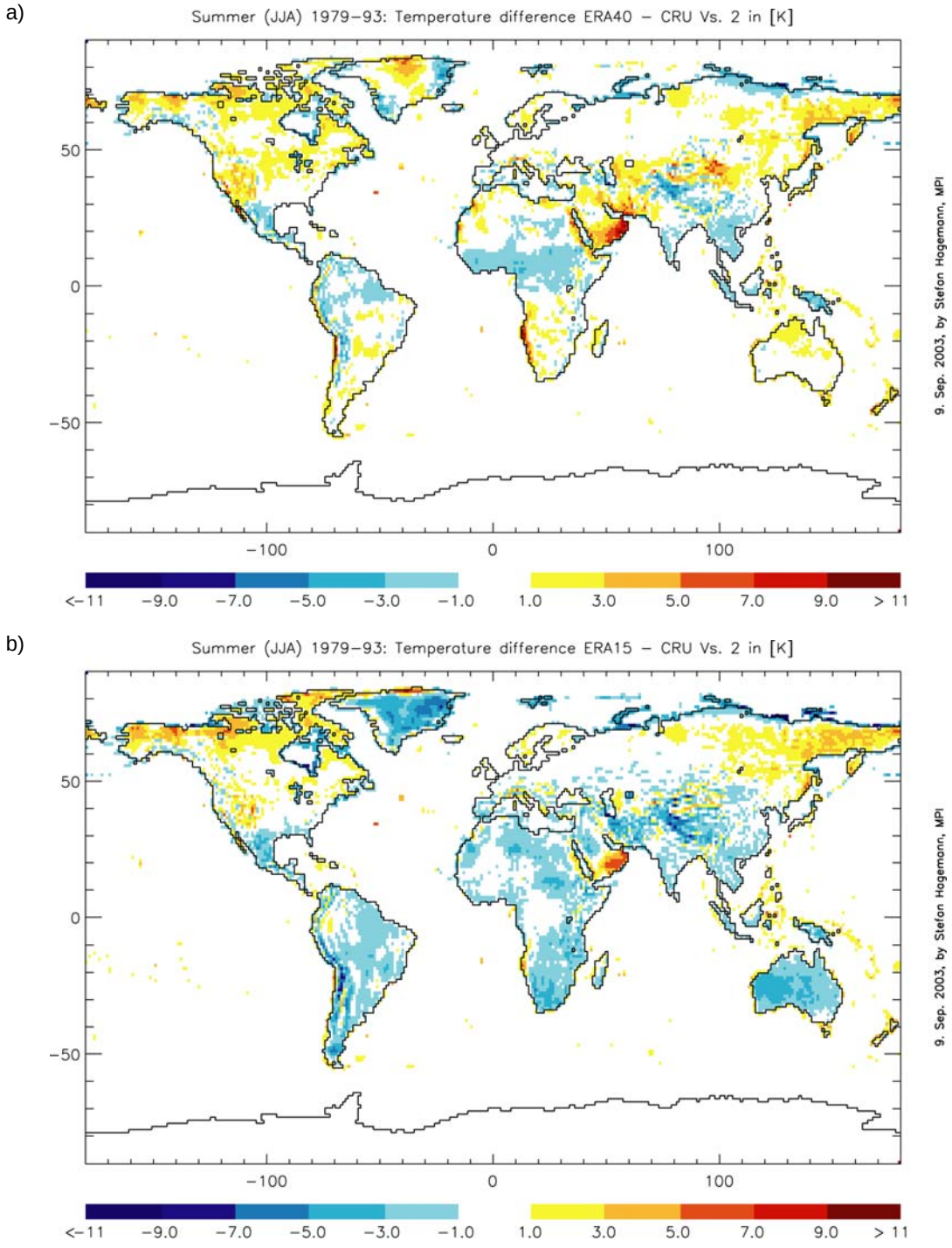

Figure 22. 2m temperature difference in the summer (JJA) 1979-93 of a) ERA40 and CRU2 data, and b) ERA15 and CRU2 data at T106 degree resolution in K.

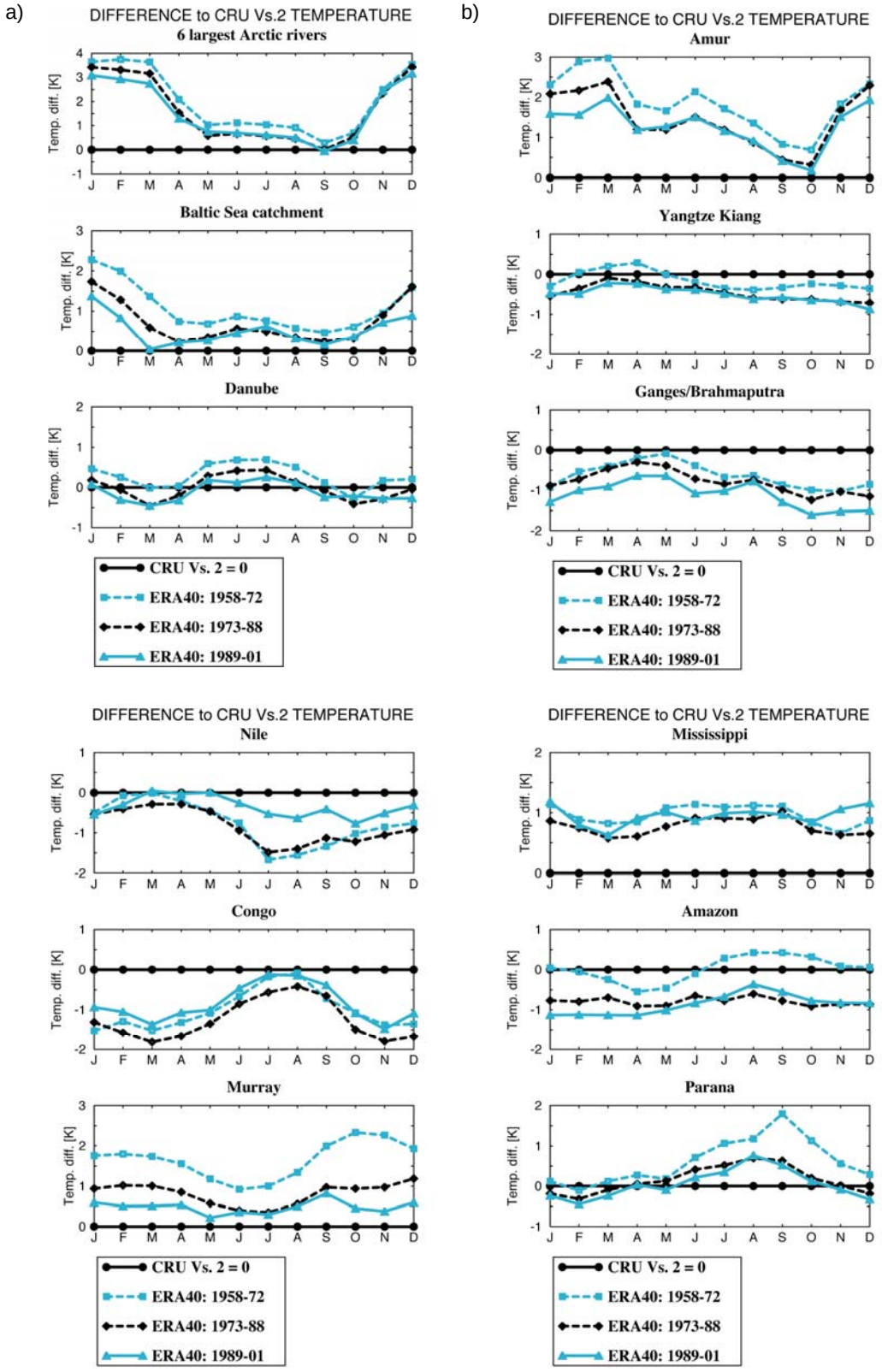

Figure 23. 2m temperature difference to CRU2 data over selected catchments in a) Arctic Ocean catchment and Europe, b) Asia, c) Africa and Australia, d) North and South America

5.3 Snowpack

In Figure 24, the ERA40 snowpack is compared to ERA15 data and the snow data climatology (SDC) of Foster and Davy (1988). ERA15 generally underestimates the snowpack in all catchments considered. In ERA40, this low bias is completely gone over 6 largest Arctic rivers (Figure 24a), the Amur and the Mississippi catchment (Figure 24b), and it is slightly improved over the Baltic Sea catchment (Fig. 24a). Only over the Danube catchment (Figure 24a) the low bias is slightly worsened.

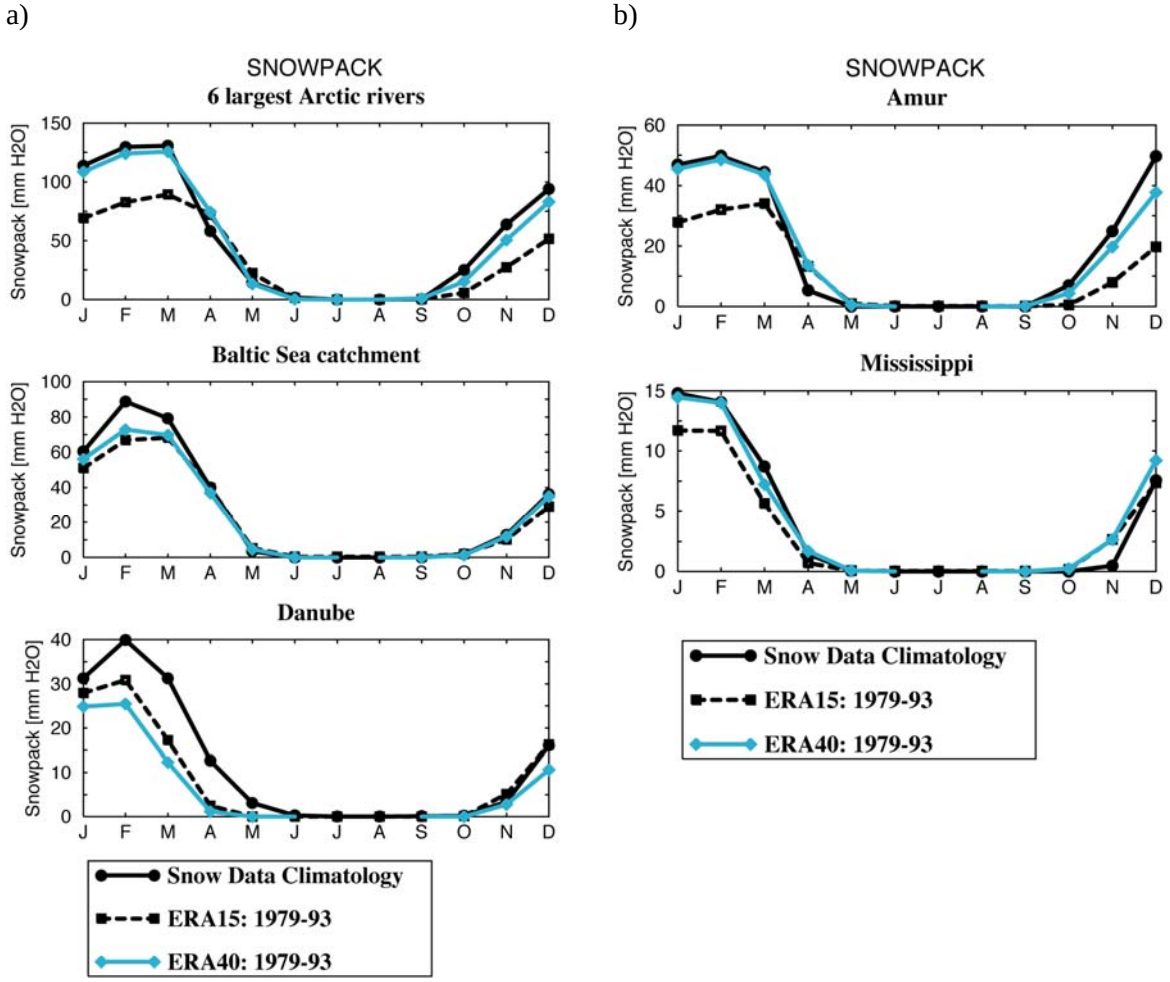

Figure 24. Accumulated snowpack (snow water equivalent) over selected catchments

In Figure 25, the ERA40 snowpack is considered for the three periods. In general it seems that less snowpack is calculated during the latest period than during the two earlier periods which leads to an underestimation of the snowpack, such as it is shown for the 6 largest Arctic rivers, the Baltic Sea catchment (Figure 25a) and the Mississippi (Figure 25b). In the intermediate period, the largest snowpack is calculated which generally agrees well with the SDC data except for the Mississippi catchment (Figure 25b) where the ERA40 snowpack is somewhat larger than the SDC data. In the earliest period, the snowpack in the high latitudes agrees well with the SDC data, as can be seen for the 6 largest Arctic rivers (Figure 25a), but for catchments which larger parts reaching further into warmer latitudes, the snowpack tends to be underestimated, such as for the Baltic Sea catchment (Figure 25a) and the Mississippi (Figure 25b).

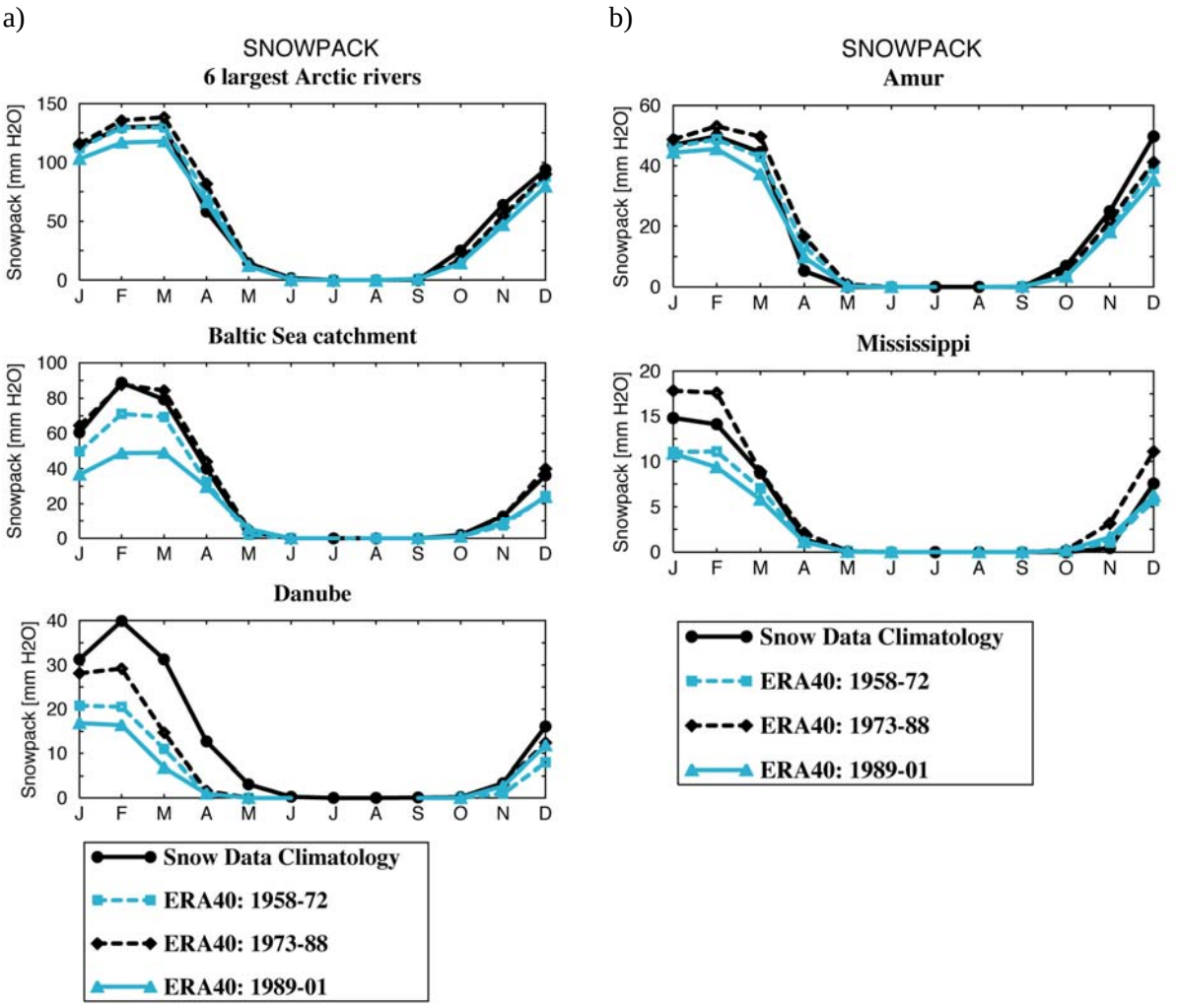

Figure 25. Accumulated snowpack (snow water equivalent) over selected catchments

5.4 Integrated water vapour content

Hagemann et al. (2003a) have derived vertically integrated water vapour (IWV) values from GPS measurements of GPS signal delay for the four months of January/July 2000/2001. They have compared these IWV values to the IWV from the ECMWF operational analyses with a special focus on the monthly averaged difference (bias) and the standard deviation of daily differences. This comparison shows that the GPS derived IWV values are well suited for the validation of operational analyses of IWV. A repetition of this comparison with ERA40 IWV values (Hagemann et al., 2003b) did not lead to significantly different results. For most GPS stations, the IWV data agree quite well with the analyses indicating that they are both correct at these locations. Larger differences for individual days are interpreted as errors in the analyses. The network of GPS stations is too sparse to identify any global bias but certain larger regions can be considered where several stations exists. Here, a dry bias in winter was found over central USA, Canada and central Siberia suggesting a systematic analysis error. Larger differences mainly exists in mountain areas. These were related to representation problems and interpolation difficulties between model height and station height. In addition, the IWV comparison can be used to identify errors or problems in the observations of the GPS signal delay. This includes errors in the data itself, e.g. erroneous outliers in the measured time series, as well as systematic errors that affect all IWV values at a specific station. Such stations were excluded from the intercomparison.

Figure 26 shows the global monthly means of IWV for the whole ERA40 period. Here, a large trend (dashed line) can be observed as well as some strange behaviour of IWV around 1972-1978. It seems that certain errors are introduced in the IWV by the first satellite data that enter the ERA40 data assimilation between 1972 and 1978.

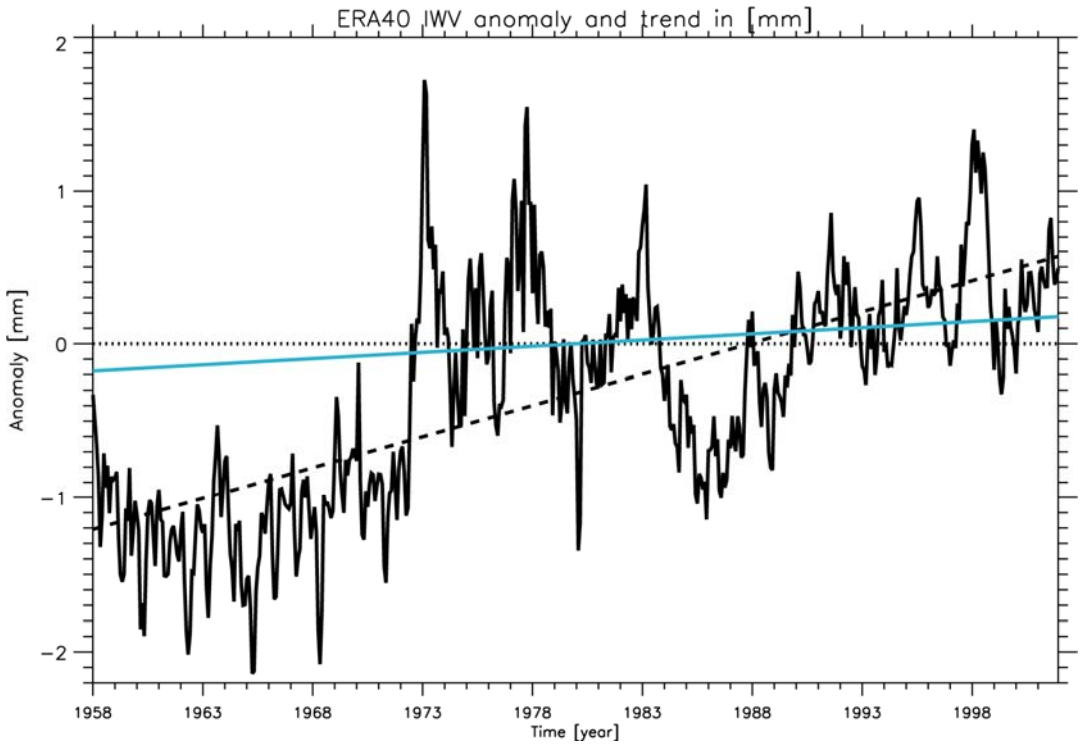

Figure 26. Vertically integrated water vapour, IWV, of ERA40 for the period 1958-2001. The dashed line shows an increasing trend. The full line indicates a corrected trend obtained by adding a factor to the data for the period 1958-1972 obtained by Bengtsson et al. (2004a), and by excluding data for the years 1972-1978.

Bengtsson et al. (2004a) have shown that the significantly lower IWV values within the earliest ERA40 period are mainly related to the availability of a different observing system than in the later 2 streams. In a sensitivity experiment with the ERA40 system, all satellite data were excluded from the data assimilation to mimic the observing system available in the earliest ERA40 period (Bengtsson et al., 2004b). The experiment was conducted for the two winters (DJF) 1990/91 and 2000/2001 as well as for the summer (JJA) 2000. The experiments yielded that the global mean of IWV was reduced by about 4.3% compared to the ERA40 control run. The most likely explanation is that the earlier incomplete observing system underestimated IWV due to the influence of the ERA40 model bias (Bengtsson et al., 2004a). In the present day observing system (in 2000/2001, see above), the model bias is suppressed by the assimilated data. Here, as mentioned above, the IWV generally agrees well with the GPS measurements (Hagemann et al., 2003b). A correction of the mean IWV before 1972 (compensating the 4.3% reduction obtained in the sensitivity experiment) brings the average trend down from 0.405 mm/decade to 0.155 mm/decade. Here, the years 1972-1978 were excluded from the trend calculation due to the data problem mentioned above.

5.5 Precipitation variability in the ITCZ

In this short section on precipitation variability we focus on the Intertropical Convergence Zone (ITCZ) over the eastern Pacific and over Africa.

Figure 27 shows the development of precipitation in the ITCZ over the eastern Pacific (140°W - 110°W) for the whole ERA40 period in the boreal summer (JJA) and winter (DJF). Here, the ERA40 precipitation has a

large variability. Before 1970, the position of the ITCZ is located further north than after that year. From 1991 onwards, the precipitation has increased considerably (such as for the global precipitation over the ocean, cf. Sect. 3.1), perhaps with a northward shift. This increase appears not only at the position of the ITCZ at around 10°N but also at a secondary ITCZ at around 10°S. These changes are not at all seen in the GPCP data (Figure 28). Note that despite of a large overestimation of precipitation in ERA40, the positioning of the two very strong El Niño events in 1982/83 and 1997/98 is captured quite well.

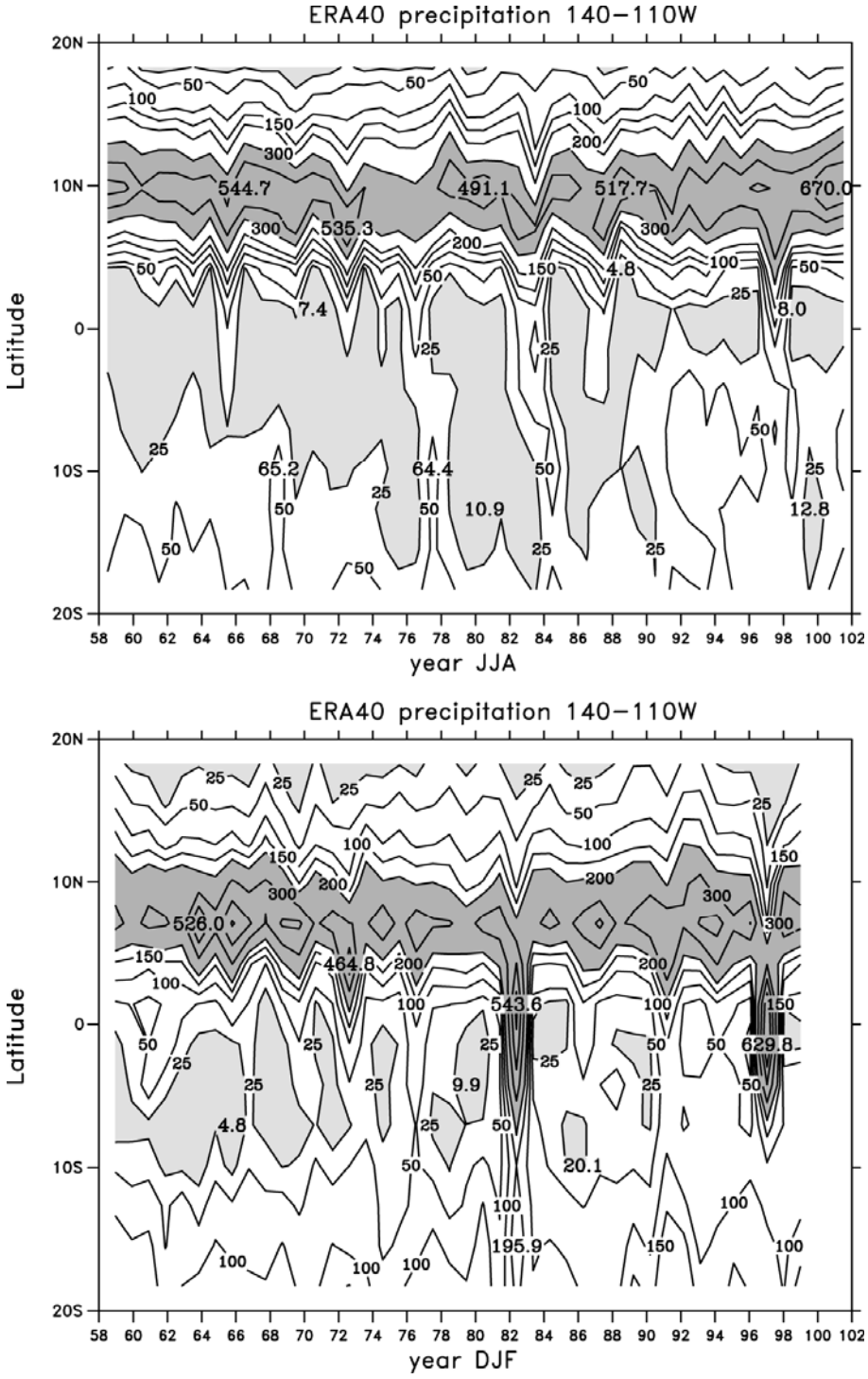

Figure 27. ERA40 precipitation in the ITCZ over the eastern Pacific (140°W - 110°W) for the whole ERA40 period in the summer (JJA) and winter (DJF). Unit: mm/month

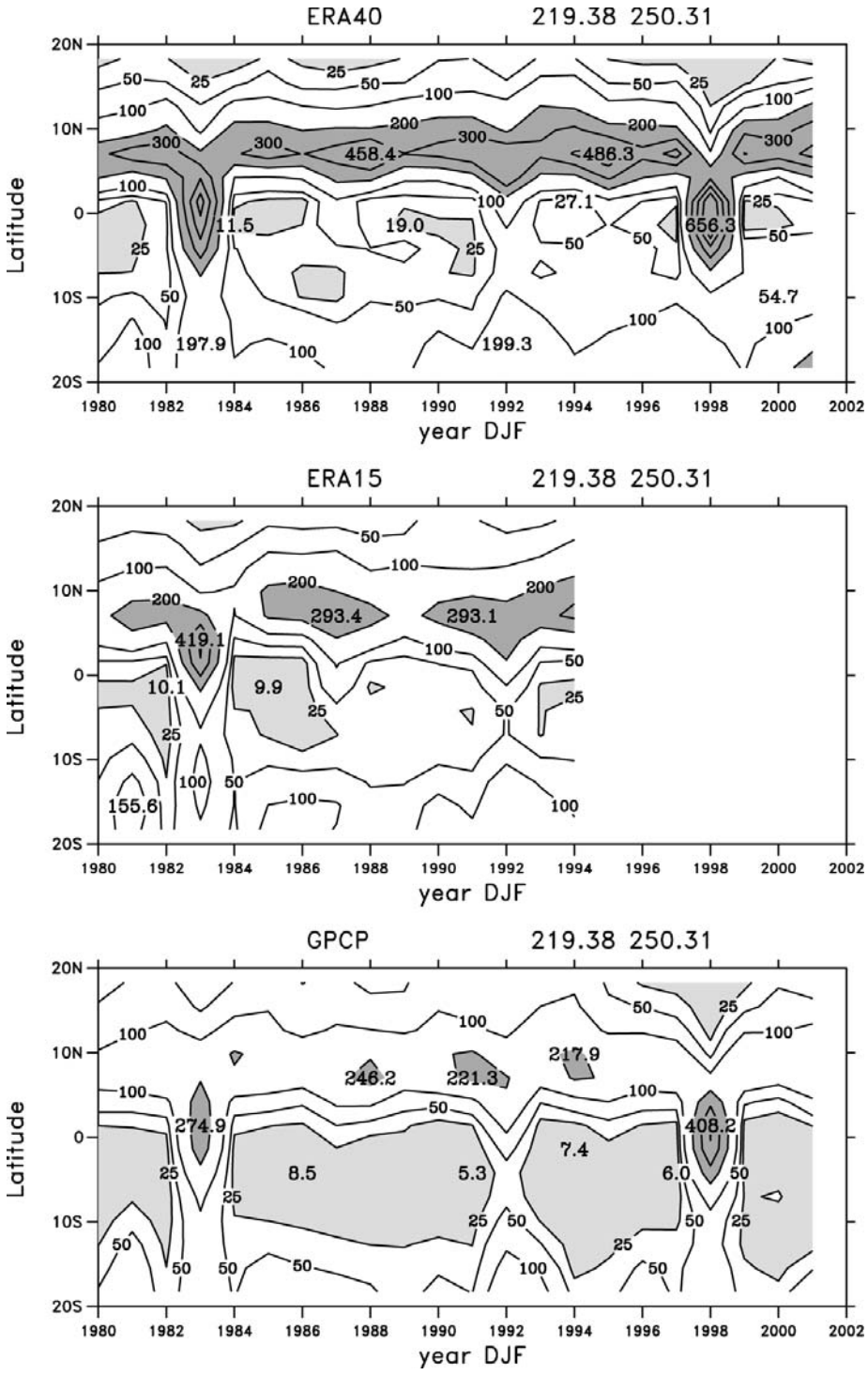

Figure 28. Precipitation of ERA40 (upper panel), ERA15 (middle panel) and GPCP (lower panel) in the ITCZ over the eastern Pacific (140°W - 110°W) for 1979-2001 in the winter (DJF). Unit: mm/month

Trends in the precipitation over the equatorial eastern Pacific go hand in hand with increases of relative humidity in the lower troposphere (Figure 29). An increase of the relative humidity around 1987 is most likely connected with the introduction of satellite observations because the relative humidity reported by SHIP observations rather suggest a decrease for the 1980s.

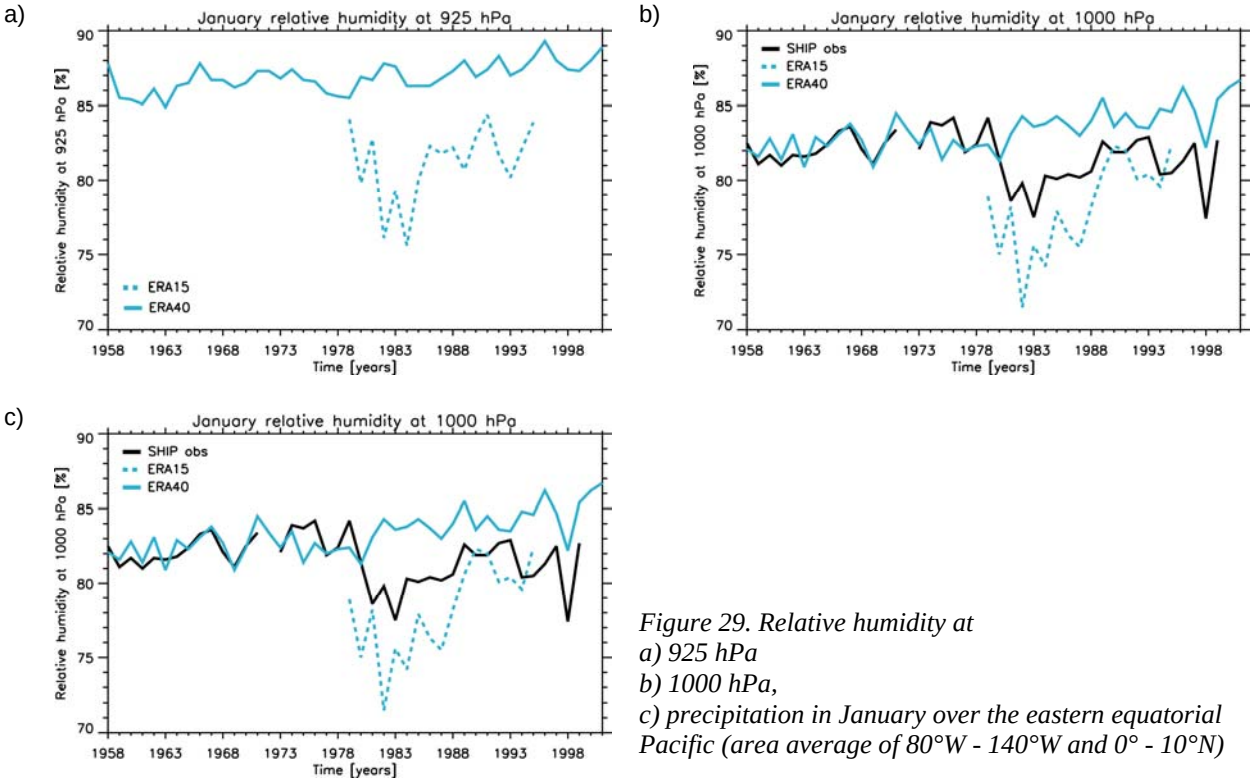

Figure 29. Relative humidity at
a) 925 hPa
b) 1000 hPa,
c) precipitation in January over the eastern equatorial Pacific (area average of 80°W - 140°W and 0° - 10°N)

In the ITCZ over tropical Africa (10°W - 20°E), very strong changes occur in the ERA40 precipitation shown in Figure 30 for the whole ERA40 period. During the first 2 years the precipitation at the ITCZ is strongly reduced compared to the long term mean, however, during JJA the ITCZ is migrating further to the north. This migration stays up to 1966 together with a reduced precipitation. Between 1967 and 1986 the precipitation is enhanced compared to the long term mean with a pronounced maximum in 1977/78 followed by an abrupt decrease in 1979. In 1998 a negative bias develops again, however, only during JJA. None of these marked changes can be seen in any of the datasets based on precipitation related observations such as CRU and GPCP (Figure 31 and Figure 32). However, the CRU dataset is based on very few observational data in this area. Also the ERA40 analysis is based on only few radiosonde data and the number of stations varies strongly. The increase of precipitation from 1967 onward nearly coincides with missing TEMP observations (3 out of 5) in the area from 1966 onward. The decrease of precipitation from 1987 onwards coincides with the introduction of SSMI observations into the ERA40 data assimilation. The change from very high to moderately high values in 1979 occurs at a time when the number of radiosonde stations increased from 1 to 3. The negative bias from 1998 onwards does not coincide with any known change in the observational data. An even stronger change of ERA15 precipitation in 1988 (Figure 31) in the same area was never understood (Stendel and Arpe, 1997), and has disappeared in ERA40.

For both summer and winter, a strong variability of the vertical profiles of the temperature in the main areas of precipitation can be found (not shown). Generally a more stable atmosphere occurs at times of higher precipitation which is the opposite of what would be expected if the static stability is the forcing factor for the precipitation. Comparing the vertical temperature profiles for selected sites and months with TEMP observations suggests that the ERA40 profiles are hardly forced by the observations.

In summary, the ERA40 data show a large variability and too much precipitation of the ITCZ over the eastern Pacific. Over tropical Africa the variability of ERA40 precipitation is unrealistic.

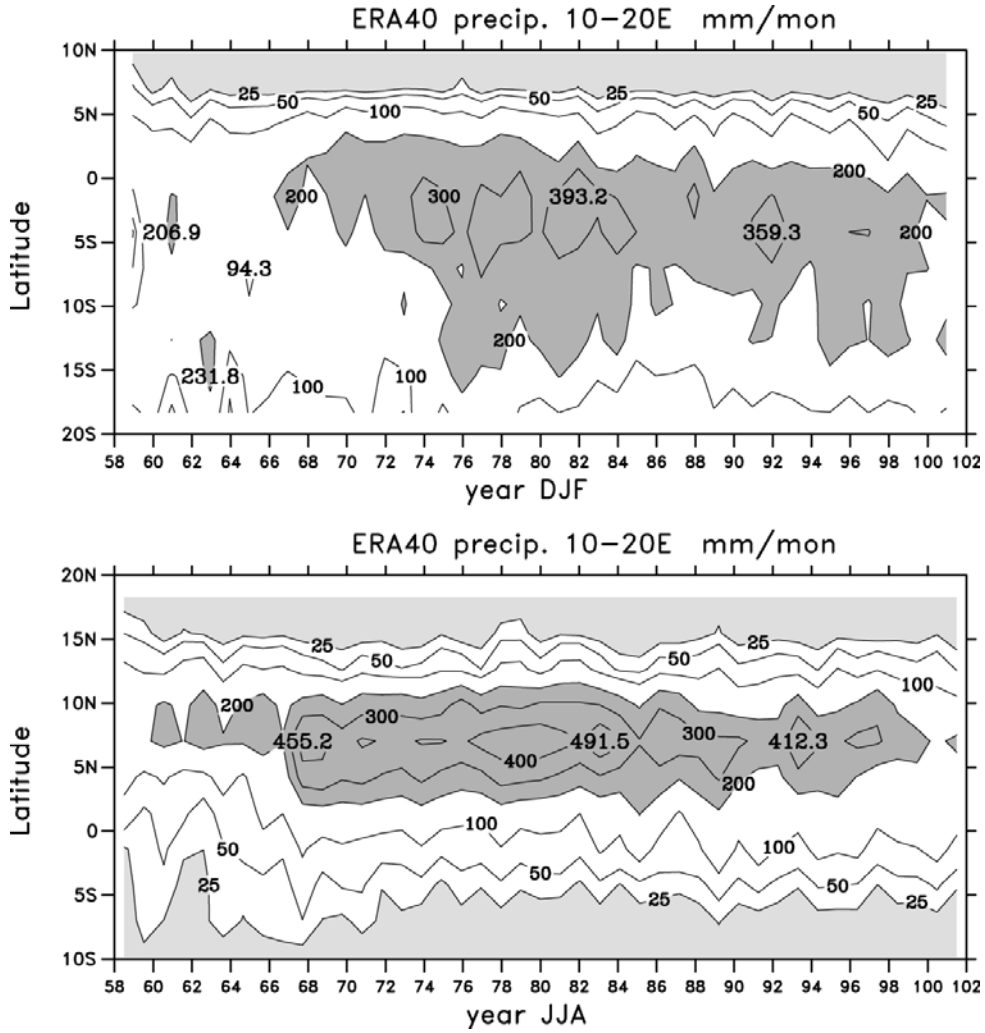

Figure 30. ERA40 precipitation in the ITCZ over Africa (10°W - 20°E) for the whole ERA40 period in the winter (DJF) and summer (JJA). Unit: mm/month

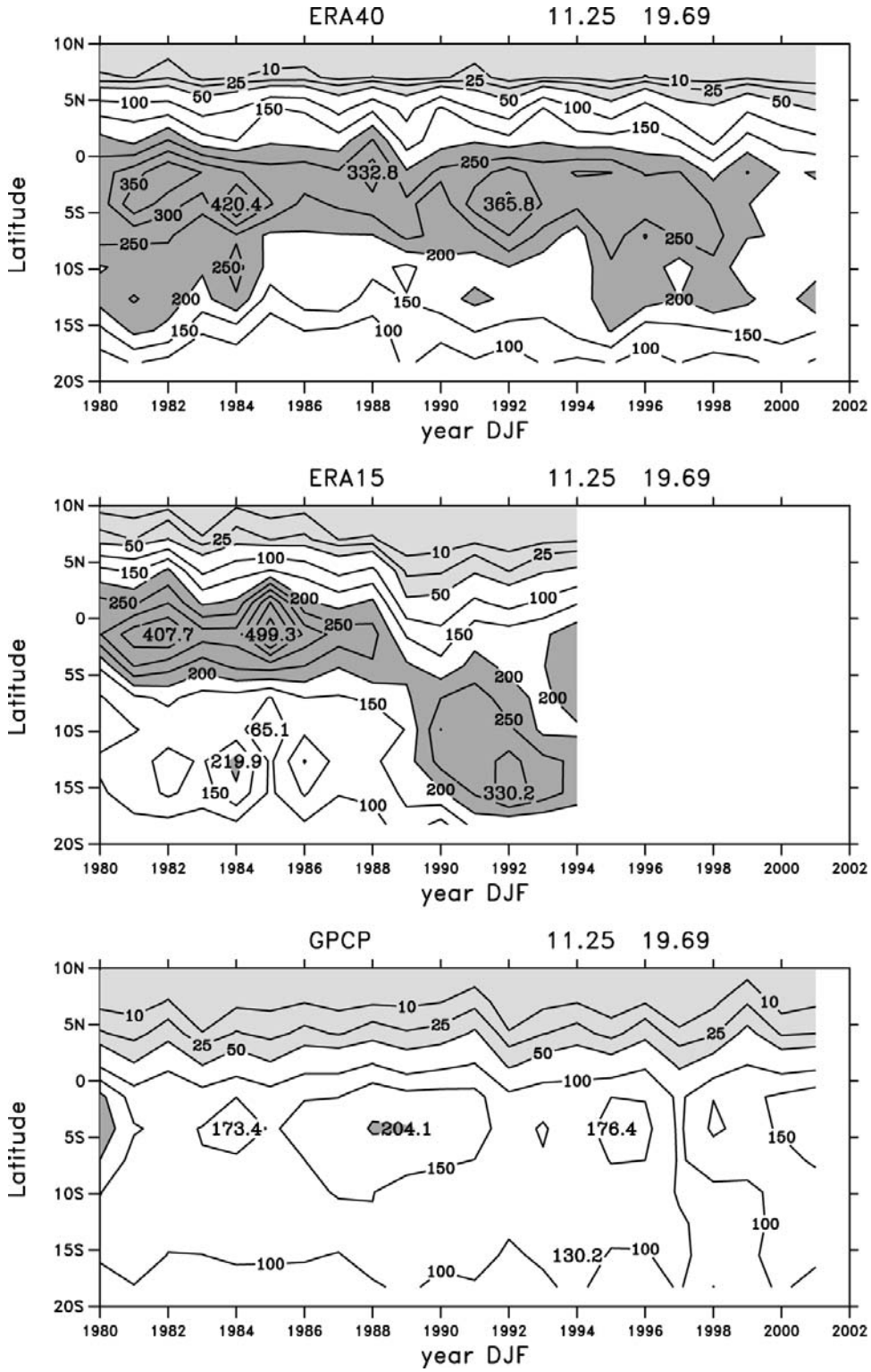

Figure 31. Precipitation of ERA40 (upper panel), ERA15 (middle panel) and GPCP (lower panel) in the ITCZ over Africa (10°W - 20°E) for 1979-2001 in the winter (DJF). Unit: mm/month

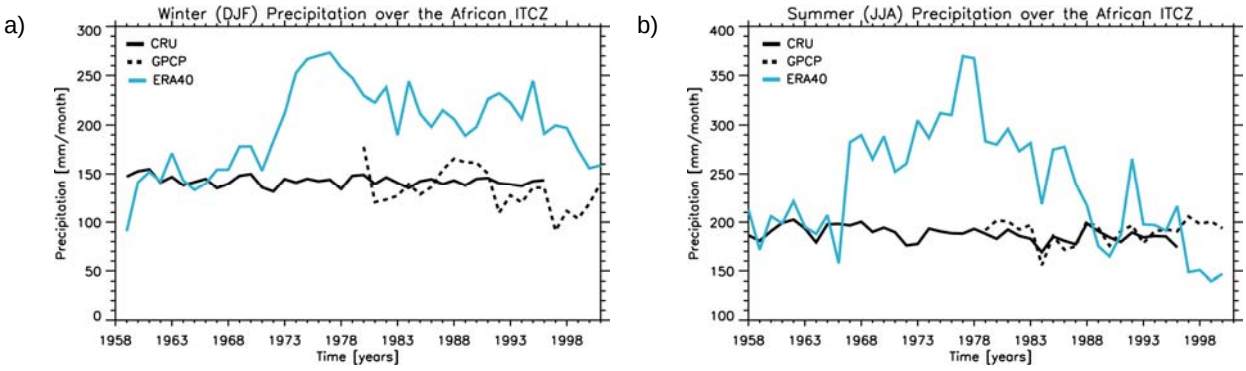

Figure 32. Precipitation over the African ITCZ in a) the boreal winter (area average of 15°E - 25°E and 0° - 10°S) and b) the boreal summer (area average of 15°E - 25°E and 5°N - 10°N). Unit: mm/month

6. Conclusions

In this study, strengths and weaknesses of the ERA40 hydrological cycle have been outlined. These should be appreciated in studies where hydrological ERA40 data are involved. Compared to the previous ERA15 re-analysis, the ERA40 hydrological cycle has changed in several respects. Its representation over land has generally improved in ERA40. These improvements comprise the removed dry bias in winter over Europe, the reduced occurrence of negative P-E values and a more realistic distribution of the snowpack. The latter generally agrees well with the snow data climatology of Foster and Davy (1988) except for Europe where the snowpack seems to be somewhat underestimated, especially in the satellite period. The severe cold bias in the ERA15 2m temperature during winter and spring over northern Eurasia has been corrected in ERA40, even though in some places now a warm bias can be seen. The smaller winter cold bias over the southern hemisphere is almost eliminated.

In spite of these improvements several deficiencies of the ERA40 hydrological cycle can be observed. The most significant deficiency is the overestimation of tropical precipitation over the ocean in the satellite and transition periods. Due to this overestimation, the long term mean of P-E over the ocean becomes positive (and not negative as it should be). Further deficiencies comprise the unbalanced global water budget, an overestimation of evapotranspiration over many river catchments, so that the corresponding P-E is often underestimated, and a general dry bias over North America which is most severe in the earliest period.

These biases in the hydrological cycle differ between the three periods as the ERA40 hydrological cycle is strongly influenced by the different observational data entering the assimilation. Therefore, hydrological trends should not be directly derived from ERA40. For IWV, tropospheric MSU temperature and global kinetic energy, Bengtsson et al. (2004a) suggested a method to correct for biases introduced by the different observing systems. Here, further analysis is required for which ERA40 variables this method may be used to avoid the detection of spurious trends related to biases connected with the availability of different observations.

In a previous study, Hagemann and Dümenil Gates (2001) analysed the hydrological cycle at the land surface of ERA15 and NCEP re-analyses for the ERA15 period 1979-1993. It was shown that both reanalyses have some deficiencies. Several of these deficiencies still exist in ERA40. The purpose of the re-analyses was to get a realistic representation of the atmosphere. Processes near the surface or in the soil were only of secondary interest, so that a realistic representation of soil processes was not required. Nevertheless, these processes influence the atmospheric circulation through their impact on the physical processes (surface fluxes) in the ERA40 model. Therefore an improvement of the land surface representation is strongly suggested for future re-analyses. This suggestion is supported by results obtained with a simplified land

surface scheme. Using the SL scheme (Hagemann and Dümenil Gates, 2003) it was possible to derive improved values of evapotranspiration and runoff from ERA40 precipitation and 2m temperature that are consistent with the ERA40 data.

Note that the biases in the hydrological cycle may also have influenced other ERA40 fields. This is at least the case for the large positive precipitation bias over the tropical oceans that has affected the circulation. Overestimated tropical precipitation amounts are working as a heat source and enhance the Hadley and Walker circulation in the atmosphere. Thus, more subsidence over land will occur which may lead to drier conditions resulting in less precipitation. In ERA40, this effect is seen in the winter over Brazil and in the summer over the Sahel zone. An even stronger effect was seen in a nudging experiment with the GCM ECHAM4.5 (Roeckner et al., 1996) where the GCM at T106 resolution was nudged with ERA40 dynamical atmospheric data (vorticity, divergence, temperature, surface pressure) for the period from January 1989 to February 1991 (Hagemann et al., 2002). In the nudged ECHAM4.5 simulation the enhanced circulation, which entered the simulation via the nudging, caused an intensification of the model's inherent dry bias over Brazil and central Africa. This indicates that in ERA40 the effect described above may be partially counteracted by the data assimilation where moisture is added to the atmosphere at each analysis cycle (see also Sect. 3.1).

In this study it was shown that some components of the ERA40 hydrological cycle have significant biases. Therefore the hydrological cycle should not be considered as quasi-observational such as it is the case for many other meteorological parameters in ERA40.

Acknowledgements

We thank Norbert Kreitz from the European Centre of Medium Range Weather Forecast for technical support in accessing the ERA40 data from the MARS archive. We are also in great debt to the ERA40 team who patiently tried to help making sense of our findings. This study was supported by funding from the European Union within the ERA40 project (contract No. EVK2-CT-1999-00027 ERA-40).

References

Andersson, E., P. Bauer, A. Beljaars, F. Chevallier, E. Hólm, M. Janiscová, P. Kållberg, G. Kelly, P. Lopez, A. McNally, E. Moreau, A. Simmons, J.-N. Thépaut, and A. Tompkins, Assimilation and modeling of the hydrological cycle in the ECMWF forecasting system. Bull. Amer. Met. Soc., in press, 2004.

Baumgartner, A., and E. Reichel, The world water balance, Elsevier, Amsterdam, 1975.

Bengtsson, L., S.Hagemann, and K. I. Hodges, Can Climate Trends be Calculated from Re-Analysis Data?, J. Geophys. Res., 109, No. D11111, doi: 10.1029/2004JD004536, 2004a.

Bengtsson, L., K. I. Hodges and S. Hagemann, Sensitivity of Re-Analyses to the Observing System: Determination of the Global Atmospheric Circulation from Reduced Observations, Tellus 56A, 456-471, 2004b

Betts, A. K., J.H. Ball, M. Bosilovich, P. Viterbo, Y. Zhang, and W.B. Rossow, Intercomparison of water and energy budgets for five Mississippi sub-basins between ECMWF Reanalysis (ERA-40) and NASA-DAO fvGCM for 1990-1999. J. Geophys. Res., 108 (D16), 8618, dot: 10.1029/2002 JD003127, 2003a.

Betts, A. K., J.H. Ball, and P. Viterbo, Water and energy budgets for the Mackenzie river basins from ERA-40. J. Hydrometeor., 4, 1194-1211, 2003b.

Bromwich, D.H., S.-H. Wang, and A.J. Monaghan, ERA-40 representation of the arctic atmospheric moisture budget, ECMWF ERA-40 Proj. Rep. Ser. 3, 287-297, 2002.

Courtier, P., E. Andersson,W. Heckley, J. Pailleux, D. Vasiljevic, M. Hamrud, A. Hollingsworth, F. Rabier, and M. Fisher, The ECMWF implementation of three dimensional variational assimilation (3D-Var). Part I: Formulation. Quart. J. Roy. Meteor. Soc., 124, 1783-1808, 1998.

Déry, S.J., and E.F. Wood, Teleconnection between the Arctic Oscillation and Hudson Bay river discharge. Geophys. Res. Lett., 31, L18205, doi:10.1029/2004GL020729, 2004.

Dümenil Gates, L., S. Hagemann, and C. Golz, Observed historical discharge data from major rivers for climate model validation, Max-Planck-Inst. für Meteorol. Rep. 307, Hamburg, Germany, 2000.

Foster, D.J., and R.D. Davy, Global snow depth climatology, USAFETAC/TN-88/006, Scott Air Force Base, Ill., 1988.

Genthon, C., Climate and surface mass balance of the Polar ice sheets in ERA40/ERA15, ECMWF ERA-40 Proj. Rep. Ser. 3, 299-316, 2002.

Gibson, J.K., P. Kållberg, S. Uppala, A. Hernandez, A. Nomura and E. Serrano, Era description, ECMWF Reanal. Proj. Rep. Ser. 1, Eur. Cent. for Medium-Range Weather Forecasting, Geneva, 1997.

Graßl, H., V. Jost, R. Kumar, J. Schulz, P. Bauer and P. Schlüssel, The Hamburg ocean-atmosphere parameters and fluxes from satellite data (HOAPS): a climatological atlas of satellite-derived air-sea-interaction parameters over the oceans, Max-Planck-Inst. für Meteorol. Rep. 312, Hamburg, Germany, 2000.

Hagemann, S., Entwicklung einer Parameterisierung des lateralen Abflusses für Landflächen auf der globalen Skala, Max-Planck-Inst. für Meteorol. Examensarb. 52, Hamburg, Germany, 1998.

Hagemann, S., K. Arpe, L. Bengtsson and I. Kirchner, Validation of precipitation from ERA40 and an ECHAM4.5 simulation nudged with ERA40 data, 3. Workshop on Re-analysis, 5-9 November 2001, ERA-40 Project Report Series, Reading, UK, 211-227, 2002.

Hagemann, S., L. Bengtsson and G. Gendt, On the determination of atmospheric water vapor from GPS measurements, J. Geophys. Res., 108, No. D21, 4678, doi: 10.1029/2002JD003235, 2003a.

Hagemann, S., L. Bengtsson and G. Gendt, Determination of atmospheric water vapour from GPS measurements and ECMWF Operational Analyses, URSI Special Symposium on Atmospheric Remote Sensing using Satellite Navigation Systems, 13-15 Oct. 2003, Matera, Italy, 2003b.

Hagemann, S., and L. Dümenil, A parameterization of the lateral waterflow for the global scale, Clim. Dyn., 14, 17-31, 1998.

Hagemann, S., and L. Dümenil Gates, Validation of the hydrological cycle of ECMWF and NCEP reanalyses using the MPI hydrological discharge model, J. Geophys. Res., 106, 1503-1510, 2001.

Hagemann, S., and L. Dümenil Gates, Improving a subgrid runoff parameterization scheme for climate models by the use of high resolution data derived from satellite observations, Clim. Dyn., 21, 349-359, 2003.

Hagemann, S., R. Jones, O.B. Christensen, M. Deque, D. Jacob, B. Machenhauer and P.L. Vidale, Evaluation of water and energy budgets in regional climate models applied over Europe, Clim. Dyn., 23, 547-567, DOI: 10.1007/s00382-004-0444-7, 2004.

Hortal, M., and A.J. Simmons, Use of reduced Gaussian grids in spectral models. Mon. Wea. Rev., 119, 1057-1074, 1991.

Huffman, G.J., R.F. Adler, A. Arkin, A. Chang, R. Ferraro, A. Gruber, J. Janowiak, R.J. Joyce, A. McNab, B. Rudolf, U. Schneider and P. Xie, The Global Precipitation Climatology Project (GPCP) combined precipitation data set, Bull. Amer. Meteor. Soc., 78, 5-20, 1997.

Kållberg, P., Aspects of the re-analysed climate, ECMWF Reanal. Proj. Rep. Ser. 2, 89 pp., Eur. Cent. for Medium-Range Weather Forecasting, Geneva, 1997.

Kalnay, E., M. Kanamitsu, R. Kistler, W. Collins, D. Deaven, L. Gandin, M. Iredell, S. Saha, G. White, J. Woollen, Y. Zhu, M. Chelliah, W. Ebisuzaki, W. Higgins, J. Janowiak, K.C. Mo, C. Ropelewski, A. Leetmaa, R. Reynolds, and R. Jenne, The NCEP/NCAR Reanalysis Project. Bull. Amer. Meteor. Soc., 77, 437-471, 1996.

Kanamitsu, M., W. Ebisuzaki, J. Woollen, S.-K. Yang, J.J. Hnilo, M. Fiorino, and G.L. Potter, NCEP-DOE AMIP-II Reanalysis (R-2). Bull. Amer. Meteor. Soc., 83, 1631-1643, 2002.

Kattan, Z., J.Y. Gac, and J.L. Probst, Suspended sediment load and mechanical erosion in the Senegal basin — Estimation of the surface runoff concentration and relative contributions of channel and slope erosion, J. Hydrol., 92, 59-76, 1987.

Latif, M., E. Roeckner, M. Botzet, M. Esch, H. Haak, S. Hagemann, J. Jungclaus, S. Legutke, S. Marsland, U. Mikolajewicz, Reconstructing, Monitoring, and Predicting Decadal-Scale Changes in the North Atlantic Thermohaline Circulation with Sea Surface Temperature, J. Climate, 17, 1605-1613, 2003.

Legates, D.R., and C.J. Willmott, Mean seasonal and spatial variability in gauge-corrected, global precipitation, Int. J. Climatol., 10, 111-127, 1990.

Li, H., A. Robock, S. Liu, X. Mo and P. Viterbo, Evaluation of reanalysis soil moisture simulations using updated chinese soil moisture observations, J. Hydrometeor., in press., 2004

Martin, E., Validation of alpine snow in ERA-40, ECMWF ERA-40 Proj. Rep. Ser. 14, 25pp, 2004.

New, M, M. Hulme and P. Jones, Representing twentieth-century space-time climate variability. Part II: Development of 1901-96 monthly grids of terrestrial surface climate, J. Climate, 13, 2217-2238, 2000.

New, M., D. Lister, M. Hulme and I. Makin, A high-resolution data set of surface climate over global land areas, Climate Res., 21, 1-25, 2002.

Roeckner, E., K. Arpe, L. Bengtsson, M. Christoph, M. Claussen, L. Dümenil, M. Esch, M. Giorgetta, U. Schlese, U. Schulzweida, The atmospheric general circulation model ECHAM-4: model description and simulation of present-day climate, Max-Planck-Inst. für Meteorol. Rep. 218, Hamburg, Germany, 1996

Rudolf, B., H. Hauschild, W. Rüth and U. Schneider, Comparison of rain gauge analyses, satellite-based precipitation estimates and forecast model results, Adv. Space. Res., 7, 53-62, 1996.

Rudolf, B., and F. Rubel, Global Precipitation. Chapter 11 of Hantel, M., Ed. (2005), Observed Global Climate, Landolt-Boernstein (Numerical Data and Functional Relationships), Springer-Verlag. in preparation, 2005.

Schubert, S., C-K. Park, C-Y. Wu, W. Higgins, Y. Kondratyeva, A. Molod, L. Takacs, M. Seablom and R. Rood, A multi-year assimilation with the GEOS-1 system: Overview and results. NASA Tech. Rep. Series on Global Modelling and Data Assimilation, Ed. M.J. Suarez, 6, 183pp., 1995

Seneviratne, S.I, P. Viterbo, D. Lüthi and C. Schär, Inferring changes in terrestrial water storage using ERA-40 reanalysis data: The Mississippi river basin, J. Climate, 17, 2039-2057, 2004.

Serreze, M.C. and A.J. Etringer, Representation of Arctic precipitation in ERA-40, ECMWF ERA- 40 Proj. Rep. Ser. 3, 317-331, 2002.

Simmons, A. J. and J. K. Gibson, The ERA-40 Project Plan, ERA-40 Project Report Series, 1, 63pp, ECMWF, Shinfield Park, Reading, UK, 2000.

Stendel, M. and K. Arpe, Evaluation of the hydrological cycle in reanalyses and observations. ECMWF Reanal. Proj. Rep. Ser. 6, 53p., 1997.

Trenberth, K.E., D.P. Stepaniak, J.W. Hurrell and M. Fiorino, Quality of reanalyses in the tropics. J. Climate 14, 1499-1510, 2001.

Uppala, S., Observing system performance in ERA, ECMWF Reanal. Proj. Rep. Ser. 3, 261 pp., Eur. Cent. for Medium-Range Weather Forecasting, Reading, UK, 1997.

Uppala, S.M., P.W. Kållberg, A.J. Simmons, U. Andrae, V. da Costa Bechtold, M. Fiorino, J.K Gibson, J. Haseler, A. Hernandez, G.A. Kelly, X. Li, K. Onogi, S. Saarinen, N. Sokka, R.P. Allan, E. Andersson, K. Arpe, M.A. Balmaseda, A.C.M. Beljaars, L. van de Berg, J. Bidlot, N. Bormann, S. Caires, A. Dethof, M. Dragosavac, M. Fisher, M. Fuentes, S. Hagemann, E. Hólm, B.J. Hoskins, L. Isaksen, P.A.E.M. Janssen, A.P. McNally, J.-F. Mahfouf, R. Jenne, J.-J. Morcrette, N.A Rayner, R.W. Saunders, P. Simon, A. Sterl, K.E. Trenberth, A. Untch, D. Vasiljevic, P. Viterbo and J. Woollen, The ERA-40 Re-analysis, ECMWF ERA-40 Proj. Rep. Ser., in press, 2004

van den Hurk, B.J.J.M., P. Viterbo, A.C.M. Beljaars, and A.K. Betts, Offline validation of the ERA40 surface scheme, ECMWF Tech. Memo. 295, 42 pp., Eur. Cent. for Medium-Range Weather Forecasting, Reading, UK, 2000.

Viterbo, P., and A.K. Betts, Impact on ECMWF forecasts of changes to the albedo of the boreal forests in the presence of snow, J. Geophys. Res., 104, 27,803-27,810, 1999.

Viterbo, P., A.C.M. Beljaars, J.-F. Mahfouf, and J. Teixeira, The representation of soil moisture freezing and its impact on the stable boundary layer, Q. J. R. Meteorol. Soc., 125, 2401-2426, 1999.

Xie, P., and P. Arkin, Global precipitation: A 17-year monthly analysis based on gauge observations, satellite estimates and numerical model outputs, Bull. Amer. Meteor. Soc, 78, 2539-2558, 1997.

Zipser, E.J., and R.H. Johnson, Systematic errors in radiosonde humidities a global problem? Preprints, 10th Symp. on Meteorological Observations and Instrumentation, Phoenix, AZ, Amer. Meteor. Soc., 72-73, 1998.